

**PERMEABILITY PREDICTION
USING NUCLEAR MAGNETIC RESONANCE**

BY

**BENJAMIN JACOB ADILLAH
PETROLEUM ENGINEERING
11538**

DISSERTATION SUBMITTED IN PARTIAL FULFILMENT OF THE
REQUIREMENTS FOR THE BACHELOR OF ENGINEERING (HONS)
(PETROLEUM ENGINEERING)
MAY 2012

SUPERVISOR
MR. ELIAS BIN ABLLAH

UNIVERSITI TEKNOLOGI PETRONAS
BANDAR SERI ISKANDAR
31750 TRONOH
PERAK DARUL RIDZUAN

CERTIFICATION OF APPROVAL

PERMEABILITY PREDICTION
USING NUCLEAR MAGNETIC RESONANCE

by
Benjamin Jacob Adillah

A project dissertation submitted to the
Petroleum Engineering Programme
Universiti Teknologi PETRONAS
In partial fulfilment of the requirement for the
BACHELOR OF ENGINEERING (Honours)
(PETROLEUM ENGINEERING)

Approved by,

(Mr. Elias Abllah)

UNIVERSITI TEKNOLOGI PETRONAS
TRONOH, PERAK
May 2012

CERTIFICATION OF ORIGINALITY

This is to certify that I am responsible for the work submitted in this project, that the original work is my own except as specified in the references and acknowledgements, and that the original work contained herein have not been undertaken or done by unspecified sources or persons.

BENJAMIN JACOB ADILLAH

Table of Contents

List of Figures.....	v
Abstract	vi
Acknowledgement	vii
Chapter 1: Introduction	1
1.1 Background	1
1.2 Problem Statement.....	1
1.3 Objective	2
1.4 Scope Of Study.....	3
1.5 Relevancy Of Project	3
1.6 Feasibility Of Project.....	3
Chapter 2: Literature Review	4
2.1 Basics of NMR Logging	4
2.2 Carr, Purcell, Meiboom And Gill (CPMG) Sequence.....	12
2.3 Rock and Fluid Properties Determination From NMR Logs.....	15
2.4 Direct Measurement of Rock and Fluid Properties Using NMR Spectrum from Cores.....	16
2.4.1 G.R Coates et al. Findings	16
2.4.2 A.K. Moss et al. (Sca 2001-29) Findings.....	18
2.4.3 Dr. Paul B Basan et al. (Aapg, 2003) Findings	20
2.4.4 Steve Lonnes et al. (2003).....	20
2.4.5 Christian Straley et al. Findings	21
2.4.6 Summary of Direct Measurement of Rock and Fluid Properties Using NMR Spectrum from Cores.....	22
2.5 Pore Size and Porosity	22
2.6 Permeability Prediction.....	24
2.6.1 Free Fluid or Coates Model.....	25

2.6.2	Mean T_2 Model or SDR Model	28
Chapter 3: Methodology		29
3.1	General Research Methodology	29
3.2	Progression Calender	30
3.3	Gantt Chart	31
3.4	Core Sample	32
3.4.1	Acquire Core Sample	32
3.5	Permeability Using Permeameter Porosity Meter (POROPERM)	32
3.5.1	Connections	32
3.5.2	Core Installation	32
3.5.3	Operating Mode	32
3.6	Core Analysis Using NMR (RINMR And MARAN)	36
3.7	Method of Analysis	38
Chapter 4: Results and Discussion		39
4.1	Description of NMR Spectra by Sample	39
4.2	Permeability Prediction	49
4.2.1	Coates Model	49
4.2.2	SDR Model	50
4.3	Overall Analysis	51
Chapter 5: Conclusion And Recommendation		53
5.1	Conclusion	53
5.2	Recommendation	54
Abbreviations and Nomenclatures		56
References		57

List of Figures

Figure 1: Proton Precess like a Child's Spinning Top	5
Figure 2: Proton Collision Illustration	7
Figure 3: Proton Collision Illustration 2	8
Figure 4: T ₂ Decay Rate	8
Figure 5: Natural Measure of Pore Size Distribution	10
Figure 6: Proton Alignment.....	12
Figure 7: Spin Tipping and Precession	13
Figure 8: Coates Model.....	25
Figure 9: FFI and BVI Classification.....	27
Figure 10: T ₂ Cutoff.....	27
Figure 11: SDR Model.....	28
Figure 12: Sensor Calibration.....	33
Figure 13: Tank Volume Calibration 1	34
Figure 14: Tank Volume Calibration 2	35
Figure 15: Results	36
Figure 16: NMR Imaging Schematic Diagram	37
Figure 17: MARAN ULTRA Machine.....	38
Figure 18: NMR T2 Relaxation Raw Data Sample #1	39
Figure 19: NMR T2 Relaxation Time Distributions Sample #1	39
Figure 20: T2 Cumulative Relaxation Time Distributions Sample #1	40
Figure 21: NMR T2 Relaxation Raw Data Sample #2	41
Figure 22: NMR T2 Relaxation Time Distributions Sample #2	41
Figure 23: T2 Cumulative Relaxation Time Distributions Sample #2	42
Figure 24: NMR T2 Relaxation Raw Data Sample #3	43
Figure 25: NMR T2 Relaxation Time Distributions Sample #3	43
Figure 26: T2 Cumulative Relaxation Time Distributions Sample #3	44
Figure 27: NMR T2 Relaxation Raw Data Sample #4	45
Figure 28: NMR T2 Relaxation Time Distributions Sample #4	45
Figure 29: T2 Cumulative Relaxation Time Distributions Sample #4	46
Figure 30: NMR T2 Relaxation Raw Data Sample #5	47
Figure 31: NMR T2 Relaxation Time Distributions Sample #5	47
Figure 32: T2 Cumulative Relaxation Time Distributions Sample #5	48

ABSTRACT

The accurate modelling of oil, gas, and water reservoirs depends fundamentally upon access to reliable rock permeabilities that cannot be obtained directly from downhole logs. Instead, a range of empirical models are employed and this paper will discuss several models derived from the Nuclear Magnetic Resonance data.

Nuclear Magnetic Resonance (NMR) measurements were initially made for high magnetic fields, emphasizing *time for protons to relax in the longitude manner, T_1* , for pore-size evaluation. However, modern NMR logging tools use *time for the protons to relax transversely, T_2* , measurements to make it possible and feasible for low field strengths and these measurements should be supported by core analysis.

This project will illustrate the differences in using the two different models which are the *COATES MODEL* and *MEAN TRANSVERSE RELAXATION TIME MODEL (MEAN T_2 MODEL, also known as, SDR model)* to measure and predict the permeability of samples. The result is then compared to see which permeability prediction model is most accurate.

The permeability is shown to be closely related to porosity, pore size, pore fluid properties and mineralogy. The NMR estimates permeability based on theoretical models that show that permeability increases with both increase in porosity and pore size.

ACKNOWLEDGEMENT

I am grateful to my supervisor, Mr Elias Abllah, whose encouragement, supervision and support from the preliminary to the concluding level enabled me to develop an understanding of this project. I would like to take this opportunity to thank the lab technician and also PRSB personnel for their full technical support. Thank you as well to colleagues at Universiti Teknologi PETRONAS for their advice. Not to forget, friends for their ideas and criticisms and parents for their invaluable continuous moral support throughout the project duration.

CHAPTER 1: INTRODUCTION

1.1 BACKGROUND

Well logging has been for ages the most economical way to evaluate drilled formations. Since created by the Schlumberger crew in 1927, the technology in well logging has improved the ability to determine the porosity and fractional fluid saturations. However, it was still hard to provide a systematic estimate of permeability. This is why the Nuclear Magnetic Resonance (NMR) has captured the interest of the oil and gas industry in the 1960's when researchers started to come up with solution which provide good permeability correlations.

Regrettably, the industry's interest was left hanging and waiting for nearly thirty years for a reliable downhole measurement tool for the NMR relaxation logging methods. When NUMAR introduced the new Magnetic Resonance Imaging Logging (MRIL) technology which is also a branch of NMR in 1992, this wait was over, and it was soon demonstrated that the long hoped for permeability determination could then be systematically predicted, especially in shaly sand formations.

Nonetheless, permeability was not the only petrophysical benefit provided by this new pulse-echo NMR log. Many other petrophysical parameters have been found achievable (e.g.: total porosity, saturations, viscosity etc.). With other parameters catered from one device, NMR might be the best single source logging tool for formation petrophysical properties ever created.

1.2 PROBLEM STATEMENT

Conventional logging tools such as neutron log, bulk density log, acoustic travel time porosity log, resistivity log, gamma ray log and several others are influenced by each and every component of a reservoir rock. The reservoir rocks generally consists of more matrix (rock) than pore space, and since the conventional logging tools are

influence by every component in the rock, it tends to be more sensitive to the matrix component rather than the fluids in the pore space since the volume is higher.

For example, the conventional resistivity log, while being extremely sensitive to the fluids in the pore space, cannot be regarded as a true fluid logging tool. This is because the tool is strongly influenced by the presence of conductive material or minerals in the rock matrix.

Thus, Magnetic Resonance Imaging logging (MRIL) comes into play. The MRIL tool can provide three types of information regarding fluids and it is more accurate than the conventional log as it is NOT influenced by the matrix material in the formation, making the reading purely from fluids responds. The three main types of information mentioned are:

- i. Quantities of the fluids in the rock
- ii. Type and properties of the fluids in the pore space
- iii. Size of the pore space that contains the fluids

From these, we derive or predict the permeability and we will be discussing the accuracy of permeability predictions in this project.

1.3 OBJECTIVE

- I. Predict and study the permeability using an NMR (nuclear magnetic resonance) capture tool which should not be influenced by the rock matrix. Data is analysed by means of the Coates Model and the SDR Model.
- II. Compare the results obtained from the Coates Model and the SDR Model and come up with a conclusion of which model predicts permeability with higher accuracy.

1.4 SCOPE OF STUDY

This study will be predicting permeability using two models which is the *Coates Model* and *SDR Model*. The results will be analysed and a comparison will be made to determine which model gives the best permeability prediction.

The study will also be focusing on lab applications and not field applications due to the time and equipment constraints.

1.5 RELEVANCY OF PROJECT

The NMR is a relatively new technology as compared to other logging tools. Though it is currently a quite luxurious tool to have in the logging operation, it is an essential tool and it has saved or improved many operations such as those mentioned in the Halliburton website (<http://www.halliburton.com>).

Thus, it is essential for the author to be in a position to learn about the new technologies which will benefit the author in choosing the right tools and provide the best economic return as an engineer for the future employer.

1.6 FEASIBILITY OF PROJECT

The project only studies the basic and fundamentals of NMR. Besides, all equipments and procedures needed for the experiment are readily available either in Universiti Teknologi PETRONAS or PRSB which would allow the student to complete the study on time.

With everything available, it could be said that this project is feasible to be done by a final year student within the timeframe provided.

CHAPTER 2: LITERATURE REVIEW

Nuclear Magnetic Resonance (NMR) data can be analyzed independently or in combination with other conventional data. NMR data can provide porosity, permeability, fluid type and fluid saturation in the logged zone. **(NMR Logging Principles & Applications by George R. C Oates, Lizhi Xiao, and Manfred G. Prammer)**

NMR refers to the *response of nuclei to a magnetic field*. The nuclei have a magnetic momentum, they behave like spinning mini bar magnets. These spinning magnetic nuclei interact with externally applied magnetic fields and respond in a characteristic fashion which can be exploited for measurements of petrophysical properties. **(Nuclear Magnetic Resonance Imaging – Technology of the 21st century by Kenyon, Kleinberg, Straley, Gubelin, and Morriss)**

2.1 BASICS OF NMR LOGGING

Modern NMR logging tools use large permanent magnets to create a strong static magnetic polarizing field inside the formation. The hydrogen nuclei of water and hydrocarbons are electrically charged spinning protons that create weak magnetic fields, like mini magnet bars. When a strong external magnetic field from the logging tool passes through a formation containing fluids, these spinning protons align themselves like compass needles along the magnetic field. This process, which is called polarization, increases exponentially with a time constant, T_1 , as long as the external magnetic field is applied **(The time constant for the polarizing process, T_1 is traditionally known as the spin lattice decay time. The name comes from solid state NMR, in which the crystal lattice gives up energy to spin aligned system)**. A magnetic pulse from the antenna rotates, or tips, the aligned protons into a plane perpendicular, or transverse, to the polarization field. These tipped protons immediately start to wobble or precess around the direction of the strong logging tool's magnetic field, just as a child's spinning top precesses in a gravitational field as illustrated in figure on the next page.

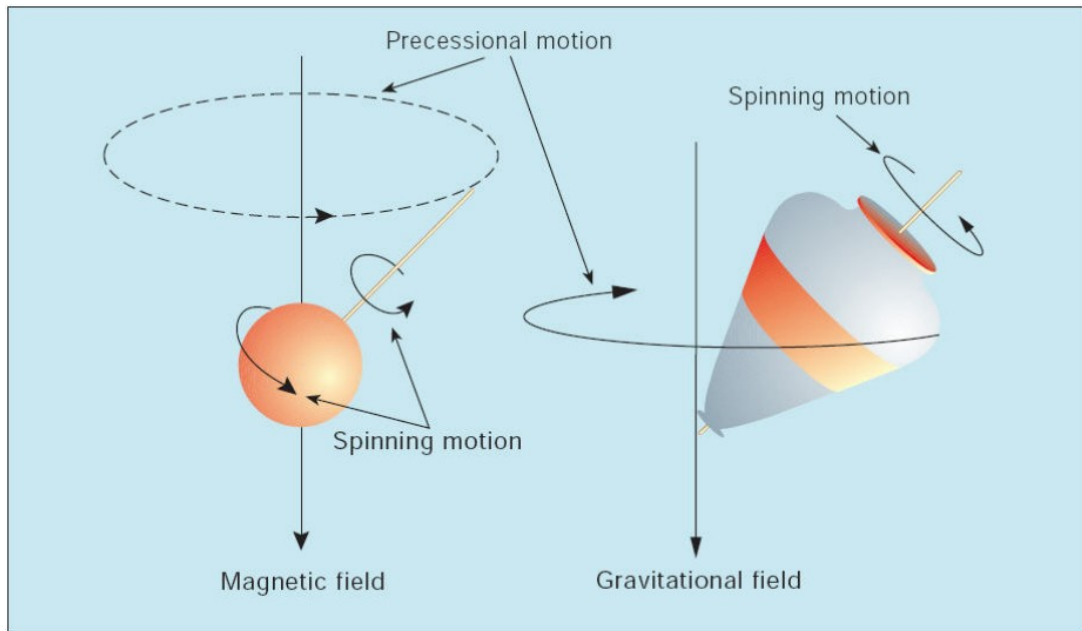


Figure 1: Proton Precess like a Child's Spinning Top

The precession frequency, **called the Larmor frequency**, is proportional to the strength of the external magnetic field. The precessing protons create oscillating magnetic fields, which generate weak radio signals at this same frequency. The total signal amplitude from all the precessing hydrogen nuclei, typically a few microvolts, is a measure of the total hydrogen content, or porosity of the formation.

The rate at which the proton precession decays is called the transverse relaxation time, T_2 , and is the second key NMR measurement because it reacts to the environment of the fluid. T_2 measures the rate at which the spinning protons lose their alignment within the transverse plane. It depends on three things:

- i. The intrinsic bulk-relaxation rate in the fluid
- ii. The surface relaxation rate which is an environmental effect
- iii. Relaxation from diffusion in a polarization field gradient which is a combination of environmental and tool effect

In addition, the spinning protons will quickly lose their relative phase alignment within the transverse plane because of variations in the static magnetic field. The observed fast decay, called the free induction decay, is due to the combined components of irreversible transverse relaxation decay interactions and the reversible

dephasing effect caused by variations in the static magnetic field. **This process is called the free induction decay, and the Carr-Purcell-Meiboom-Gill (CPMG) pulse echo sequence is used to compensate for the rapid free induction decay caused by reversible transverse dephasing effect (refer to section 2.2 for CPMG sequence in detail).** The pulse echo technique in today's tools is called the CPMG sequence, named after Carr, Purcell, Meiboom and Gill, who refined the pulse echo scheme (**Carr HY and Purcell EM: "Effects of diffusion on Free Precession in Nuclear Magnetic Resonance Experiments", Physical Review 94, No. 3, (1954):630-638, and Meiboom S and Gill D: "Modified Spin Echo Method for Measuring Nuclear Relaxation Times", The Review of Scientific Instruments 29, No. 8 (1958):688-691)**

The three components of the transverse relaxation decay time play a significant role in the use of the T_2 distribution for well logging applications. For example, the intrinsic bulk relaxation decay time is caused principally by the magnetic interactions between neighbouring spinning protons in the fluid molecules. These are often called **spin-spin interactions**.

Molecular motion in water and light oil is rapid, so, the relaxation is inefficient with correspondingly long decay time constants. However, as liquids become more viscous, the molecular motions are slower. Then, the magnetic fields, fluctuating due to their relative motion approaching the Larmor precession frequency, and the spin-spin magnetic relaxation interactions become much more efficient. Thus, tar and viscous oils can be identified because they relax relatively efficiently with shorter T_2 decay times than light oil or water.

Fluids near, or in contact with, grain surface relax at a much higher rate than the bulk fluid relaxation rate. This process is also called **Grain – surface relaxation**, and is one of the most important mechanisms for the spinning protons to lose their magnetization. This is because of complex atomic level electromagnetic field interactions at the grain surface. Molecules in fluids are always in motion and diffuse about in a pore space, there is a high probability (characterized by the surface relaxivity parameter) that the spinning proton in the fluid will relax when it encounters a grain surface. At this point, the protons may either transfer some of

their spin to the grain, contributing to T_1 , or irreversible dephase time T_2 . The speed of relaxation here partially depends on the rock type; **sandstones are generally three times more efficient than carbonates to relax hydrogen**, and the amount of magnetic minerals present in the rock; e.g. iron.

For the surface relaxation process to dominate the decay time, the spinning protons in the fluid must make multiple encounters with the surface, **caused by Brownian motion**, across small pores in the formation. They repeatedly collide with the surface until a relaxation event occurs.

The speed of relaxation depends on how often protons can collide with grains. Collisions are less frequent in large pores as they have smaller surface to volume ratio as illustrated in figure.

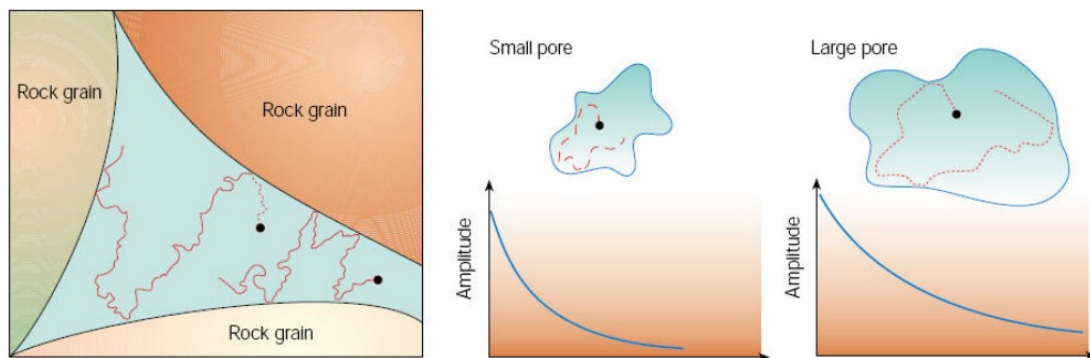


Figure 2: Proton Collision Illustration

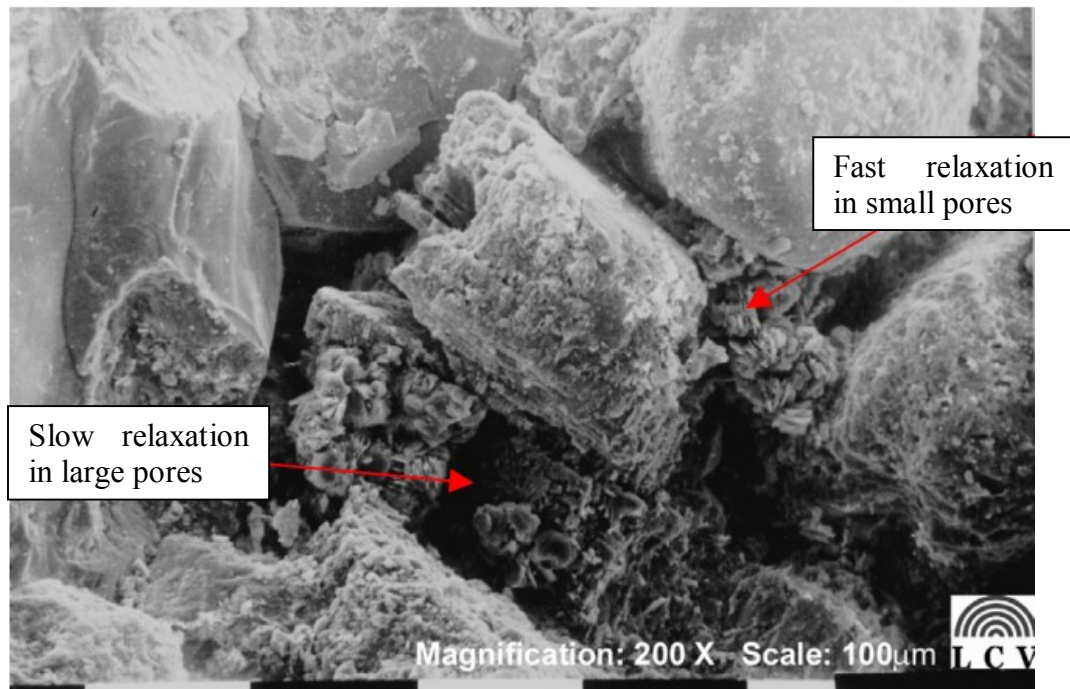


Figure 3: Proton Collision Illustration 2

Small pores have large surface to volume ratio resulting in short relaxation time T_2 and large pores have large or long T_2 decay time. In other words, the T_2 decay rate is inversely proportional to the surface to volume ratio of the rock being measured and directly proportional to the size of the pore as illustrated.

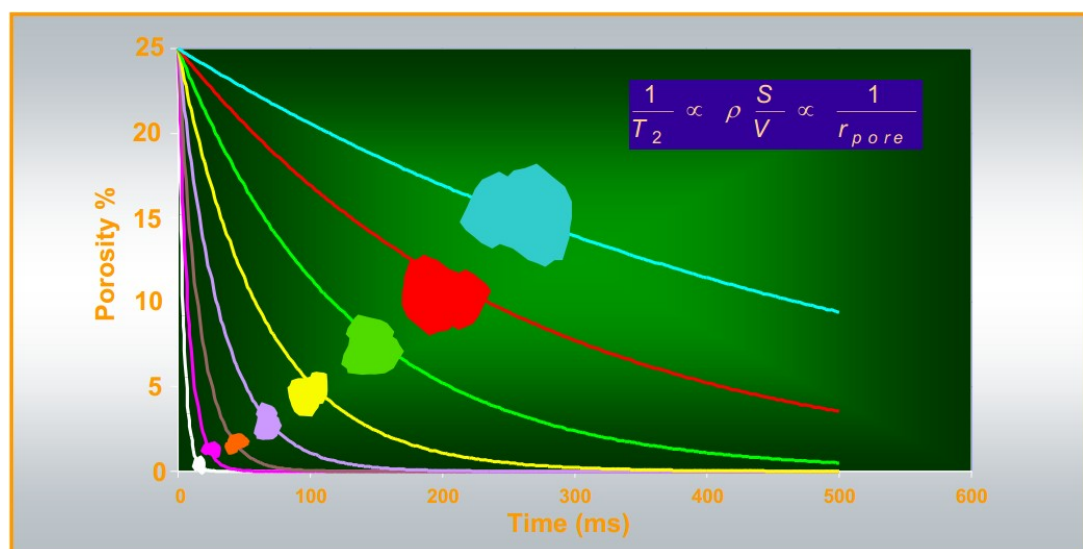


Figure 4: T_2 Decay Rate

The resulting T_2 distribution leads to a natural measure of the pore size distribution. Traditionally, the total porosity seen in formations is subdivided into three major components:

- i. Free fluid porosity with long T_2 components
- ii. Capillary bound water with T_2 greater than 3 milliseconds and less than the T_2 cutoff for the free fluid component
- iii. Fast decaying clay bound water below 3 milliseconds

As NMR tool technology has improved over the last decade with shorter echo spacing, **more components of porosity now can be measured, including the fastest clay bound water signal below 3 milliseconds.** Today, for example, the CMR-200 and CMR-Plus can measure T_2 down to the 0.3 milliseconds range while logging continuously, and the 0.1 milliseconds during stationary measurements.

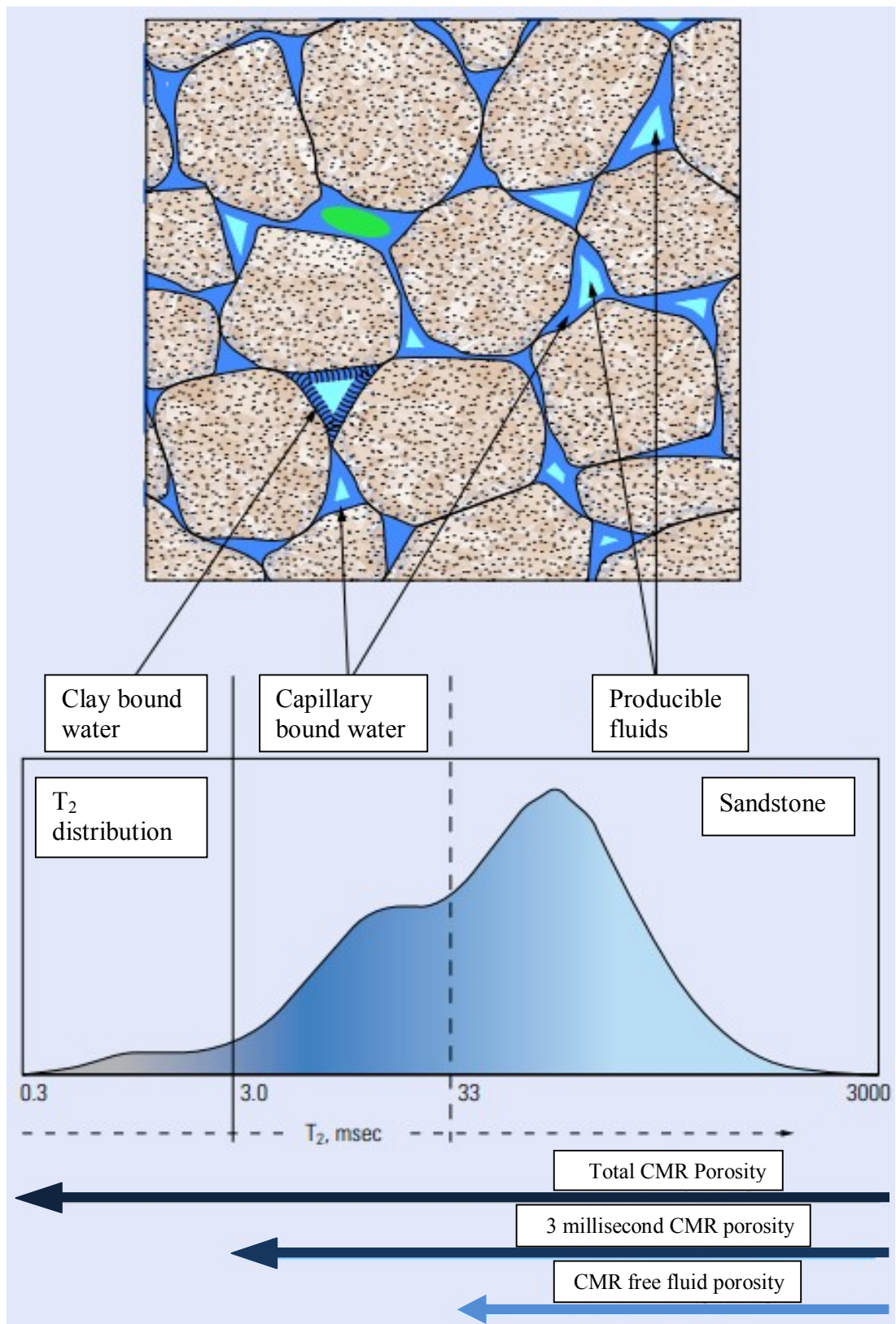


Figure 5: Natural Measure of Pore Size Distribution

In figure 5, NMR T_2 distributions (bottom) are used to identify fluid components (top) in sandstone reservoirs. In water wet sandstone rock, the T_2 time distribution reflects the pore size distribution of the formation. Producing fluids include free water (light blue), or pockets of oil (green) in the larger pores. Free water and light oils contribute to longer T_2 time components. Capillary bound water (dark blue) is held against sand grains by surface tension and cannot be produced. Clay bound water (black) is also not producible. Shorter T_2 time components are from irreducible water that is closely bound to grain surfaces.

Relaxation from diffusion in the polarization field gradient is a technique frequently used to differentiate oil from gas (**Akkurt R, Vinegar HJ, Tutunjian PN and Guillory AJ: “NMR Logging of Natural Gas Reservoirs”, The log Analyst 37, No. 6 (November-December 1996): 33-42**). As the spinning protons move randomly in the fluid, any magnetic field gradients will lead to incomplete compensation with the CPMG pulse echo sequence. The magnetic field can have two sources, the magnet configuration of the logging tools and the magnetic susceptibility contrast between grain materials and pore fluids in porous rocks.

For example, between spin flipping pulses, some protons will drift due to their Brownian motion from one region to another of different field strength, which changes their precession rate. As a result, they will not receive the correct phase adjustment for their previous polarization environment. This leads to an increase in the observed transverse dephasing relaxation rate. Gas has relatively high mobility compared with oil and water, and therefore, the spinning protons in gas have a much larger diffusion in gradient effect. It is important to know that a uniform magnetic field gradient is not required to exploit the diffusion in gradient effect. All that is required is a well defined and mapped gradient volume to differentiate gas from oil (**Flaum C, Guru U and Bannerjee S: “Saturation Estimation from Magnetic Resonance Measurements in Carbonates”, Transactions of the SPWLA 41st Annual Logging Symposium, Dallas, Texas, USA, June 4-7, 2000 Paper HHH**).

Another type of relaxation is the relaxation by bulk fluid processes. The bulk fluid effect shows that relaxation still occurs even if grain surfaces and internal field gradients are absent. This can often be neglected, but becomes significant in very large pores such as in vuggy formations or when hydrocarbons are present, wetting the grain surfaces and preventing fluid grain collisions.

2.2 CARR, PURCELL, MEIBOOM AND GILL (CPMG) SEQUENCE

For the case of logging, the NMR tool is calibrated to the magnetic resonance frequency of the hydrogen nuclei. This is because hydrogen has a relatively large magnetic momentum and is abundant in the subsurface rock formation. The Responses of the hydrogen nuclei to an outside external magnetic field and total signal amplitude are the measurements exploited with the NMR tool. Using the NMR tool, the measurement sequence is to be known. This measurements sequence is as such:

i. Proton Alignment

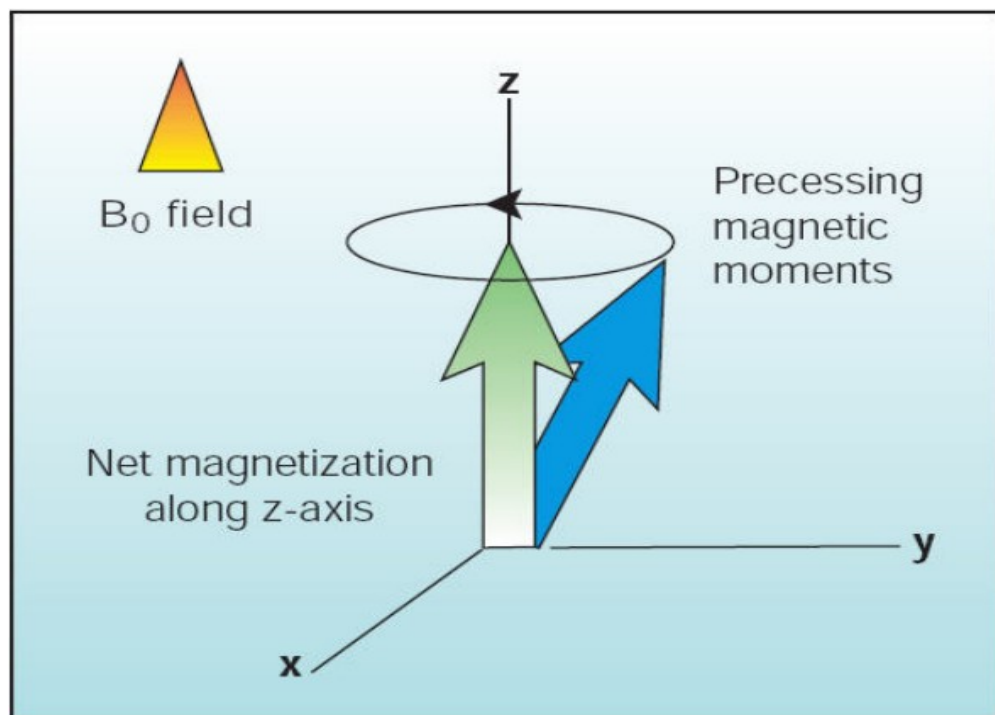


Figure 6: Proton Alignment

Protons aligned by applying a large constant magnetic field for a few seconds and the protons will remain aligned as long as the constant magnetic field

remains unchanged. However, the protons are always precessing parallel to the axis of the outside magnetic field.

ii. Spin Tipping and precession

The aligned protons are tipped through applying an oscillating magnetic field (one different than the magnetic field before). The frequency of this magnetic field is calibrated to be equal to the Larmor frequency of the hydrogen which is 2.3 MHz in a magnetic field of 550 Gauss.

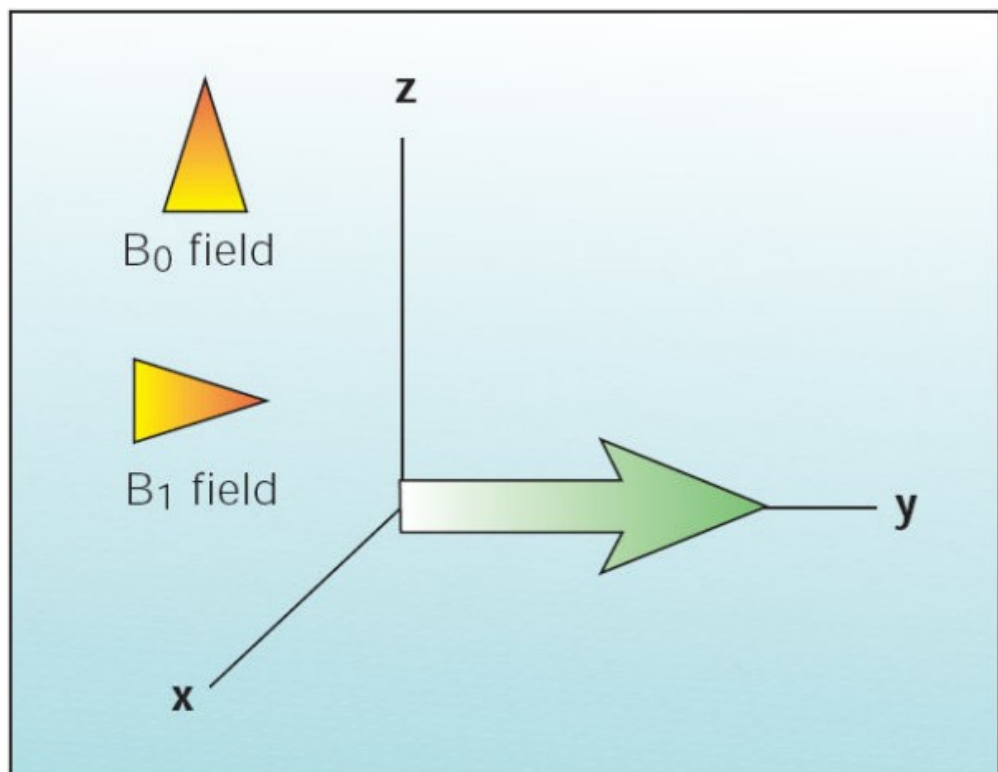


Figure 7: Spin Tipping and Precession

The magnitude of the tip angle is a function of the newly applied magnetic field and for how long the magnetic field is switched on. To obtain a 90 degrees tip angle, a field of 4 gauss switched on for 16 microseconds could be applied.

iii. **Dephasing, Free Induction Decay (FID)**

While the protons are precessing around the new magnetic field direction, the protons generate another small magnetic field which is measured by an antenna inside the NMR tool.

However, the initial magnetic field and the tipped magnetic field are not perfectly homogeneous and the protons will not precess exactly at the same frequency. Over time, the protons lose synchronization (dephase) and the decaying signal is measured. This decay time is called the **Transverse Relaxation Time, T_2** .

The decay signal is also referred as free induction decay (FID)

iv. **Refocusing**

The dephasing caused by the inhomogeneities is reversible. The protons can be refocused by introducing a new pulse which is 180 degrees to the original spin tipping pulse and should be twice as long. As the protons rephase to their original location, they generate a new signal and this is captured by the antenna and is called the **spin echo**. The spin echo also decays on the rate of the previous decay in the “**dephase**” item above. Then, the 180 degree pulses are applied repeatedly

The usual procedure is to apply 180 degree pulses in an evenly spaced train as close together as possible. The entire pulse sequence is called the **CPMG** sequence, named after their inventors; Carr, Purcell, Meiboom and Gill.

(Borehole Geophysics, Nuclear Magnetic Resonance (NMR) Logging by Professor Michael Riedel and Nuclear Magnetic Resonance Imaging – Technology of the 21st century by Kenyon, Kleinberg, Straley, Gubelin and Morriss)

2.3 ROCK AND FLUID PROPERTIES DETERMINATION FROM NMR LOGS

In principle, NMR logging is a technique sensitive to atomic scale structure and molecular motion. The NMR data acquired for rock evaluation reflects the distribution of the electrical signal generated by the hydrogen nuclei (i.e. proton) contained in the fluids saturating the rocks. NMR signal decay as function of a characteristic time constant called the spin-spin relaxation time, T_2 , which provides information about the physical and chemical environment of nuclei.

NMR logging data are also highly dependent on fluid location, fluid type, pressure, temperature and tool characteristics. From the study of *Canon, Minh and Kleinberg*, it is proposed that to quantitatively interpret the NMR logging data is to remove the field polarization correction and replace it with tailored corrections for each volume present. The advantage of this tailored correction is to yield a result independent of the acquisition parameter even in difficult cases of gas, oil based mud and vugs.

According to *Hamada, Al-Blehed and Al-Walad*, the number of hydrogen atoms in gas also depends strongly on the temperature and pressure. It is important to estimate accurately the pressure and temperature to account for their effects on NMR logging results in natural gas reservoir. To evaluate NMR logs, they suggested using T_1 contrast due to the separation of water and light hydrocarbon (oil and gas). Then the gas and oil signal were again separated based on large contrast in T_2 relaxation times.

2.4 DIRECT MEASUREMENT OF ROCK AND FLUID PROPERTIES USING NMR SPECTRUM FROM CORES

It has also been reported that the laboratory low field NMR Spectra measurements conducted on representative core samples can determine the following:

- i. Effective porosity, free fluid porosity, pore size distribution and pore geometry
- ii. Fluid saturations distributions
 - a. Free or bound fluid volumes, mobile oil, gas and water
 - b. Capillary bound water, immobile water
 - c. Clay bound water
 - d. Permeability
- iii. Producing fluids and fluid types, oil, gas and water
- iv. Oil viscosity and wettability

There are two reasons why the rock core measurement used low field NMR instrument which are;

- i. Many rocks, particularly sandstones, contain magnetic material which gives the rock a high magnetic susceptibility. This affects the measurements and results. This susceptibility effect is much reduced at low fields.
- ii. To correlate with NMR well logging tools which work at low field (1 MHz – 2 MHz).

2.4.1 G.R Coates et al. Findings

NMR measurements on core plug samples provides information about the pore space which cannot be obtained by any other non-destructive tests and are often used to calibrate and improve interpretation on NMR logs. The first NMR based comparison between core and well log data (Magnetic Resonance Imaging, MRIL) was investigated by **G.R. Coates et al.** This study is based on data from the **Conoco 33-1** test well in **Newkirk Field, Oklahoma**. Core samples are examined using a 10 MHz frequency spectrometer and the results are compared with those from the MRIL which operates at 1MHz.

From the porosity measurement, comparison made between MRI porosity to core porosity shows the MRI porosity is equal to or less than the core porosity (total porosity) over the depth interval and this might be due to several reasons:

- i. Fluid in micro pores associated with shale can have relaxation times much shorter than 3.0 milliseconds
- ii. The largest difference between MRI porosity and core porosity appears to be associated with the presence of the iron bearing minerals which can increase the efficiency of the relaxation of the atoms.

A total of 23 consolidated sandstone plugs of size 25.2 mm diameter ranged between 30 mm – 45 mm in length were used. Those samples have undergone sample preparation and routine core measurements. The core plugs were fully saturated with 30,000 ppm NaCl. Prior to NMR measurements, formation factor (FF) was determined with resistivity meter on the samples. XRD was also conducted in order to determine the mineralogy and clays content.

The NMR facility used was the **Bruker Minispec PC110 NMR** analyzer. In order to minimize evaporation of the brine during analysis, samples were wrapped in a domestic film wrap and overlapping layers of PTFE tape. The samples were then sealed inside PTFE vessel. The plugs were positioned inside the **Minispec** probe. Probe tuning setting of 90^0 and 180^0 pulses widths were carried out individually for each sample.

The result of a combined application of NMR logging and core analysis, **CorEVAL**, on reservoirs which has a low resistivity gas bearing reservoir has also been reported to yield 30% increase of gas saturation. The increment was independently validated by *Boult, Ramamoorthy, Theologou, East, Drake and Neville*. To run the NMR tool, the well must not suffer from serious borehole breakout which would otherwise affect the reading of the NMR logs.

The conclusions of the above study showed that the comparison between results obtained laboratory, **NMR Spectra**, and those obtained with the wireline log, **NMRIL/CMR**, showed a reasonable degree of agreement. The large difference in

the result is biased on the sample volume and the difference in frequency which is **2 MHz for the wireline NMR tool and 10MHz for the laboratory Minispec.**

It could be concluded that:

- i. The core experiments confirm a strong relationship between permeability and the function $T_1 \text{ s/F}$ was also observed, but the correlation was poorer
- ii. The $\log T_1$ and T_2 relationship permeability provide a reasonably consistent acceptable value, consistent in range and trend with the core permeability
- iii. The \log porosity apparently reads lower than core porosity in the presence of ferromagnetic minerals. This is a factor to be considered in applying this technology. However, the 3 milliseconds echo spacing also introduces potential pore size related sensitivity
- iv. In general, the \log relaxation times are greater than those observed for core. The core log comparisons shows considerable scatter. The differences in experimental conditions have introduced variations greater than those due to changes in petrophysical properties

2.4.2 A.K. Moss et al. (SCA 2001-29) Findings

In another investigation into the effect of clay type, volume and distribution on the NMR measurements in sandstones was conducted by **A.K Moss et al. (SCA 2001-29)**. The effect of clay type characteristic and volume on NMR T_2 spectra on synthetic sandstone packs which containing varying amount of randomly distributed montmorillonite or illite clay were investigated. The relationship was observed between the basic petrophysical properties and the T_2 spectra.

From the investigation, the findings can be summarized as follows:

- i. Synthetic sandstone samples have been used to evaluate the effect of clay on NMR measurement. This type of systematic analysis helps to relate NMR response to pore-space geometries and aids in the interpretation of NMR core and log data.
- ii. Clay type and content significantly affects the petrophysical properties and NMR relaxation responses of sandstones.

- iii. T_2 NMR measurements can detect the presence of clay microporosity and distinguish between free and bound water.
- iv. Both the tuned Coates and SDR equations successfully modelled the permeability of the clay free and montmorillonite containing samples. A different set of model parameters was needed to model the permeability of the sample containing illite clay.

A.K. Moss (Reslab UK) in his other paper titled “**NMR core plug measurements to compliment SCAL studies**” mentioned that the NMR spectrometer’s has the ability to provide a pore volume measurement early in the core test program. This is invaluable when calculating end point saturations and interpreting resistivity data for desaturated samples. Besides a single phase, NMR measurements can also be used to provide saturation information in core plugs containing two phases. Other applications of NMR measurements with SCAL programs include investigation of drilling mud filtrate particulate invasion and detection of pore structure change.

The studies have described the qualitative effects of clay content and mineralogy on NMR data and methodologies to formulate a model to estimate shale volumes from NMR core plug data. The findings are:

- i. Porosity and S_w measurement:
 - The samples studied were unconsolidated cores and they were protected in head shrinkable sleeves and PTFE end caps. The result showed that all plugs NMR porosity values are slightly higher than the helium porosity. This might be due to a small amount of bulk brine trapped between the samples and protective sleeve and also unconsolidated samples are also susceptible to deformation on application of confining stress.
 - NMR measurement can also provide an estimate of water saturation, S_w . the NMR porosity values can be used to calibrate water saturation during air or brine desaturations. The NMR derived saturations allowed the evaluation of resistivity index data and the calculation of Archie saturation exponent

ii. Drilling Mud Particulate Invasion Using NMR:

- NMR measurements is sensitive to pore geometry variation, it is an ideal technique for investigating drilling mud invasion.
- It can be assumed that the differences in NMR T₂ distributions are due to varying degrees of mud invasion.

iii. Detection of Pore Structure Change Using NMR:

- Sample plug damage by alteration of the pore geometry can be detected due to repeatedly cleaned, dried and saturated processes.

2.4.3 Dr. Paul B Basan et al. (AAPG, 2003) Findings

A study by Dr. Paul B Basan et al. (AAPG, 2003) focusing on “**Maximizing the value of NMR core data**” shows an example of how NMR core data can be used to calibrate CMR log and to define facies of a reservoir from the **Nile Delta** area. Secondly, it shows how the NMR core data can improve permeability prediction and hydrocarbon detection. Identifying facies or rock types provide a framework for mapping their distribution, which in turn helps to define the geometry of reservoir and non-reservoir bodies.

Thus, this framework is fundamental for creating a static model for predicting reservoir behaviours. On the other hand, both NMR core and log measurements provide two basic parameters which are T₂ and amplitude, which are required for rock typing.

The relationship between pore size and NMR responses links these data to a method characterizing the internal structure of rock types. The process, which is called **NMR Response Typing**, works equally well with core and log data, and adds a dimension to reservoir characterization unavailable from other techniques.

2.4.4 Steve Lonnes et al. (2003)

Steve Lonnes et al. (2003) on the study “**NMR Petrophysical Prediction on Cores**” applies common NMP petrophysical correlations to predict porosity, irreducible water saturation, S_{wi}, and permeability from 100% water saturated cores and

compares the results to the associated data generated by routine core analysis. NMR petrophysical predictions were generated from laboratory analysis on 326 plug samples of 100% water saturated plug samples. The results of the study indicated that the NMR performs well at predicting the porosity of 100% brine saturated samples. Permeability predictions differ from laboratory measured values by up to 2 orders of magnitude. S_{wi} predicted using a fixed T_2 cut off (fixed pore size cut off) differs from laboratory measured values as much as 25-30 saturation units.

In general, NMR measurements predict porosity reasonably well. S_{wi} comparison shows that the standard deviation from 1:1 line is 0.107 (10.7 saturation units). The appreciable data scatter resulting from the application of a fixed T_2 cut-off. For permeability estimation, both models generated an appreciable amount of data scatter relative to the actual permeability. The prevailing explanation for the data scatter resulting from NMR petrophysical predictions on 100% water saturated cores relates to the unknown nature of each samples surface relativity.

Practical extensions of the results suggest:

- i. The interpretation of NMR T_2 measurements as pore size distributions may lead to an incorrect petrophysical understanding
- ii. NMR logging data should be calibrated with core analysis data and not laboratory NMR measurements on core plugs
- iii. The inclusion of NMR derived petrophysical quantities in core analysis program creates the potential for petrophysical misinterpretation

2.4.5 Christian Straley et al. Findings

A paper entitled “**Core Analysis by Low Field NMR**” by **Christian Straley et al.** mentioned that new NMR logging tools use T_2 measurements made at low field strengths and these measurements should be supported by core analysis measurements. Low field NMR T_2 distributions from water saturated plugs were used to estimate producible fluids for sandstones and carbonates and to estimate clay bound water and matrix permeability. The number of samples tested in this experiment, program or finding was 192 sandstones and 71 carbonates. Their experiments demonstrated that low field NMR has been found to be more accurate in

measuring water and oil volumes than high field NMR for rocks that have large internal magnetic field gradients

2.4.6 Summary of Direct Measurement of Rock and Fluid Properties Using NMR Spectrum from Cores

In summary, NMR is capable of quantifying a wide range of petrophysical properties with one non-destructive measurement. As conclusion:

- i. NMR measurements using low magnetic fields give accurate porosity values for both sandstone and carbonates
- ii. Low field T_2 distributions show good agreement with T_1 distributions and correspond to pore size distributions from mercury porosimeter
- iii. Free fluid porosities calculated using cut offs of 33 milliseconds for sandstones and 92 milliseconds for carbonates respectively predict the producible fluids:
 - a. In sandstones, clay bound water can be estimated from T_2 distributions using a 3 millisecond cut off.
 - b. Sandstone permeability can be estimated. For some vuggy carbonates, the NMR permeability estimate is improved by excluding long T_2 porosity that is associated with the vugs.
 - c. Using D_2O (deuterium oxide, heavy water) diffusion, NMR can measure S_o and S_w in native state core. This method allows oil viscosity to be estimated in situ for water wet rocks

2.5 PORE SIZE AND POROSITY

Brownstein, K.R. and Tarr, C.E. states that the NMR behaviour of a fluid in pore space of a reservoir rock is different from the NMR behaviour of the fluid in bulk form. For example, as the size of pores containing water decreases, the difference between the apparent NMR properties of the water in the pores and the water in bulk form increases. (**Brownstein, K.R., and Tarr, C.E., 1979, Importance of Classical Diffusion in NMR Studies of Water in Biological Cells, Physical Review, Series A, v. 19.**)

Simple methods can be used to extract enough pore-size information from MRIL data to greatly improve the estimation of such key petrophysical properties as permeability and the volume of capillary-bound water. **(Sandor, R.K.J., and Looyestijn, W.J., 1995, NMR logging—the new measurement, Shell International Petroleum Maatschappij, The Hague, The Netherlands)**

Water in the micro porosity is hard to see and has a very rapid relaxation time and behaves like a solid, but modern MRIL tool can see this. Modern MRIL tool sees micro porosity which results in total porosity and not effective porosity like older NMR tools. Pore-size information supplied by the modern tools is used to calculate an effective porosity that mimics the porosity measured by the older NMR tools. **(Prammer, M.G., et al., 1996, Measurements of clay-bound water and total porosity by magnetic resonance logging, SPE 36522, 1996 SPE Annual Technical Conference and Exhibition Proceedings, v. 9 (Formation evaluation and reservoir geology))**

In addition, one of the key features of the MRIL design philosophy is that the NMR measurements of the formation made when the MRIL tool is in the wellbore can be duplicated in the laboratory by NMR measurements made on rock cores recovered from the formation. This ability to make repeatable measurements under very different conditions is what makes it possible for researchers to calibrate the NMR measurements to the petrophysical properties of interest (such as pore size which then relates to permeability) to the end user of MRIL data. **(Marschall, D., 1997, Magnetic resonance technology and its applications in the oil and gas industry, part 2, Petroleum Engineer International, v. 70, no. 4)**

The common volumetric model used in the comparison consists of a matrix component and a pore-fluid component. The matrix component is composed of clay minerals and non-clay minerals, and the pore-fluid component is composed of water and hydrocarbons. Conceptually, the pore fluids can be more finely divided into clay-bound water, capillary-bound water, movable water, gas, light oil, medium-viscosity oil, and heavy oil.

2.6 PERMEABILITY PREDICTION

The most important measurement of the NMR tool is the Permeability. The measurement of permeability allows the production rate to be predicted, allowing the optimization of the completion and stimulation programs while reducing the cost of coring and production. Permeability is derived empirically from the relationship between NMR porosity and mean values of the transverse relaxation time obtained from laboratory tests. The following formula is normally used:

$$k_{\text{NMR}} = C * (\phi_{\text{NMR}})^4 (T_{2 \log})^2$$

$T_{2 \log}$ is the logarithmic mean of the transverse relaxation time distribution, ϕ_{NMR} is the NMR porosity and k_{NMR} is the permeability. C is an empirical constant. **(Earth & Planetary Sciences, Lecture EPS-550, Professor Michael Riedel, Winter 2008)**

NMR relaxation properties of rock samples are dependent on porosity, pore size, pore-fluid properties and mineralogy. The NMR estimate of permeability is based on theoretical models that show that permeability increases with both increasing porosity and increasing pore size. **(Ahmed, U., Crary, S.F., and Coates, G.R., 1989, Permeability estimation; the various sources and their interrelationship, SPE 19604, 1989 SPE Annual Technical Conference and Exhibition Proceedings, v. 9 (Formation evaluation and reservoir geology))**

Two related kinds of permeability models have been developed. **The free-fluid or Coates model** can be applied in formations containing water and/or hydrocarbons. **The average- T_2 model or SDR** can be applied to pore systems containing only water **(Marschall, D., Gardner, J., and Curby, F.M., 1997, MR laboratory measurements—requirements to assure successful measurements that will enhance MRI log interpretation, paper SCA 9704).**

2.6.1 Free Fluid or Coates Model

The free fluid or Coates model (afterwards known as Coates model) in its simplest form predicts the permeability, k , by:

$$k = \left[\left(\frac{\Phi}{C} \right)^m \left(\frac{FFI}{BVI} \right)^n \right]$$

Where:

k = permeability

Φ = porosity

C = formation dependent coefficient

FFI = Free Fluid Index (Volume of Movable Free Fluid) where $FFI = \Phi - BVI$

BVI = Irreducible Bulk Volume (obtained through Cutoff BVI or Spectral BVI)

m = assumed to be 2-4

n = assumed to be 2

The figure below shows the Coates permeability model uses the FFI/BVI ratio to describe change in the surface to volume ratio.

Coates Model

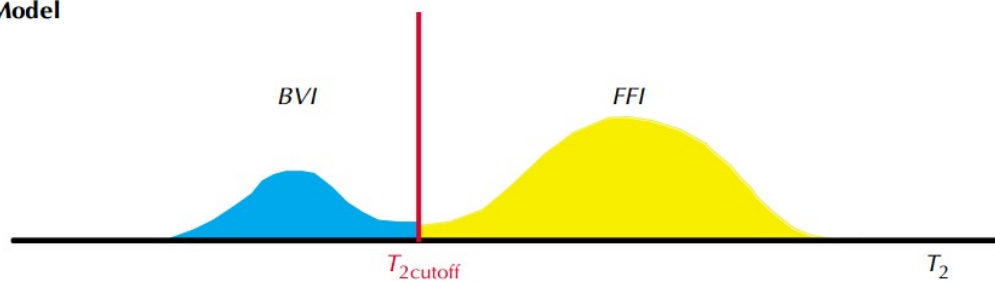


Figure 8: Coates Model

Free Fluid Index (FFI) and Bulk Volume Irreducible (BVI)

The porosity and pore size information from NMR measurements can be used to estimate both the permeability and the potentially producible fluids, or commonly known as movable fluids.

The NMR estimate of producible porosity is called the free-fluid index (MFFI or FFI). The estimate of MFFI is based on the assumption that the producible fluids reside in large pores, whereas the bound fluids reside in small pores.

A T_2 value can be selected below which the corresponding fluids are expected to reside in small pores and above which the corresponding fluids are expected to reside in larger pores. This T_2 value is called T_2 cutoff (**Timur, A., 1967, Pulsed nuclear magnetic resonance studies of porosity, movable fluid and permeability of sandstones, SPE 2045, 42nd Annual Meeting preprint, SPE. Later published in 1969 in Journal of Petroleum Technology, V. 21, no. 6, p. 775–786).**

The $T_{2 \text{ cutoff}}$ can be determined with NMR measurements on water saturated core samples. Specifically, a comparison made between the T_2 distribution of a sample in a fully water saturated state, and the same sample in a partially saturated state. (**Coates, G., et al., 1997, a new characterization of bulk-volume irreducible using magnetic resonance, paper QQ, 38th Annual SPWLA Logging Symposium Transactions, 14 p. Also published in 1997 in DiaLog (London Petrophysical Society), v. 5, no. 6, p. 9–16. Later revised and published in The Log Analyst, v. 39, no. 1, p. 51–63.)**

In simpler terms, the $T_{2 \text{ cutoff}}$ can be determined by the intersection between the T_2 of a fully saturated core with the T_2 of a desaturated core.

The T_2 distribution is composed of **movable (MFFI)** and **immovable (BVI)** components. Because pore size is the primary controlling factor in establishing the amount of fluid that can potentially move, and because T_2 spectrum is often related to pore size distribution, a fixed T_2 value should directly relate to a pore size at which below that value fluid will not move. Through the partitioning of the T_2 distributions, $T_{2 \text{ cutoff}}$ divides MPHI into free fluid index (MFFI) and bound fluid porosity, or bulk volume irreducible (BVI) as shown in the figure that follows.

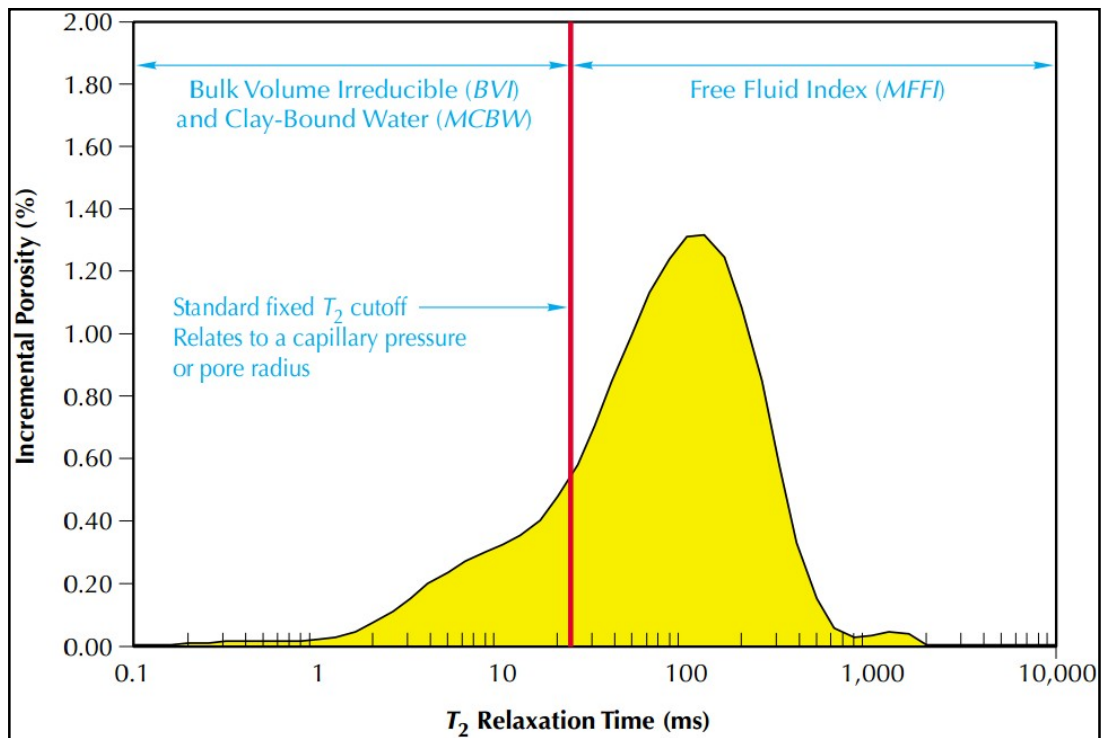


Figure 9: FFI and BVI Classification

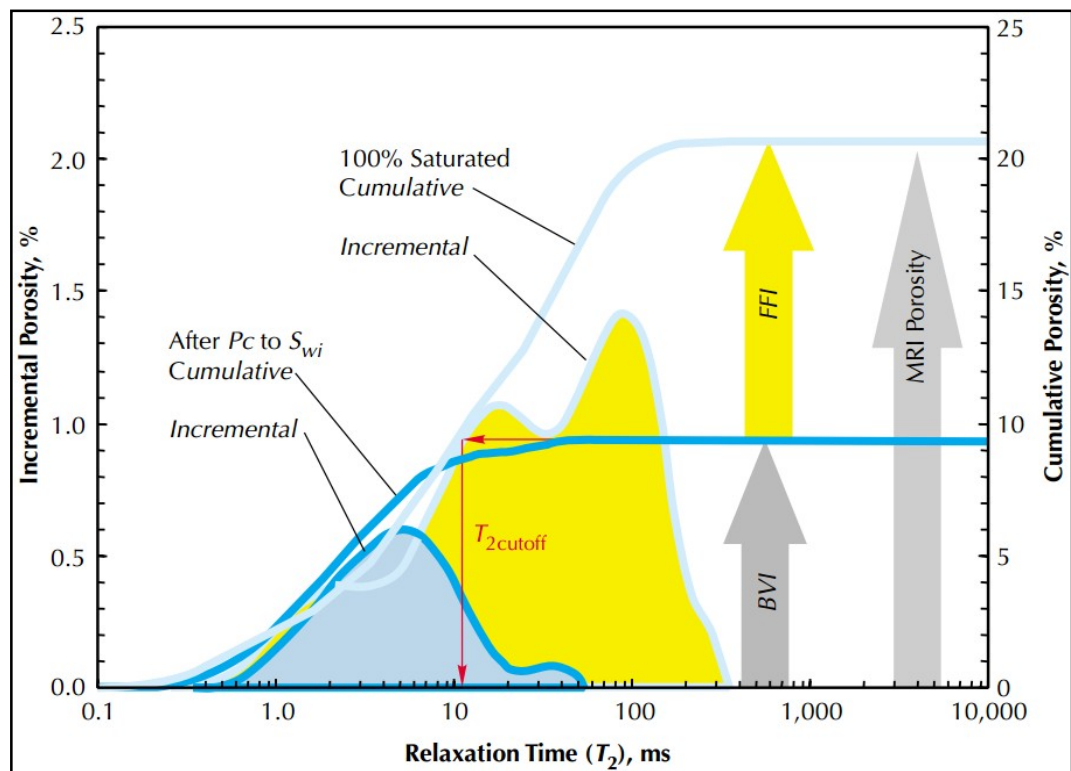


Figure 10: T_2 Cutoff

2.6.2 Mean T_2 Model or SDR Model

The Mean T_2 Model or SDR Model (afterwards known as SDR model) is shown by the formula:

$$k = a T_{2lm}^2 \phi^4$$

Where

k = permeability

a = formation dependant coefficient

T_{2lm} = logarithmic mean of T_2 distribution

ϕ = effective porosity

The SDR model can effectively be used in zones containing only water. However, if oil or oil filtrate are present, the mean T_2 value will be skewed towards the bulk liquid T_2 value and the permeability will result in a false reading. Since the effect of hydrocarbon on T_{2lm} is not correctable, the SDR model cannot be used for hydrocarbon bearing formations.

The SDR model's permeability uses an average transverse relaxation time, T_2 , value to describe changes in surface to volume ratios. This is illustrated by the figure below.

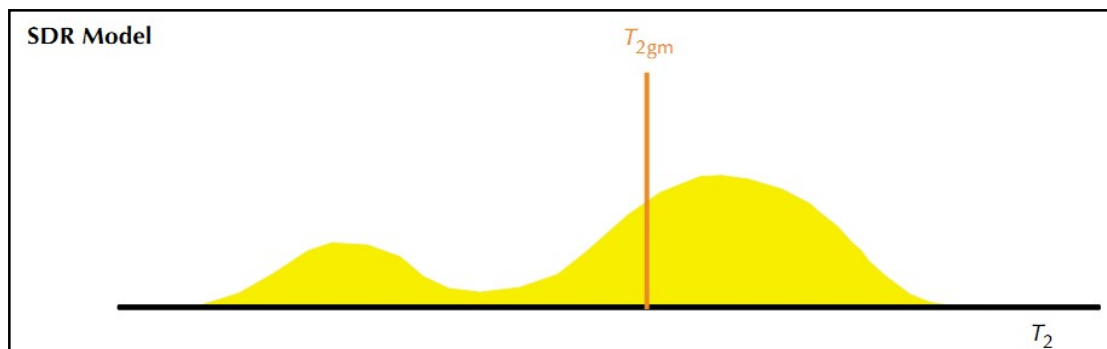
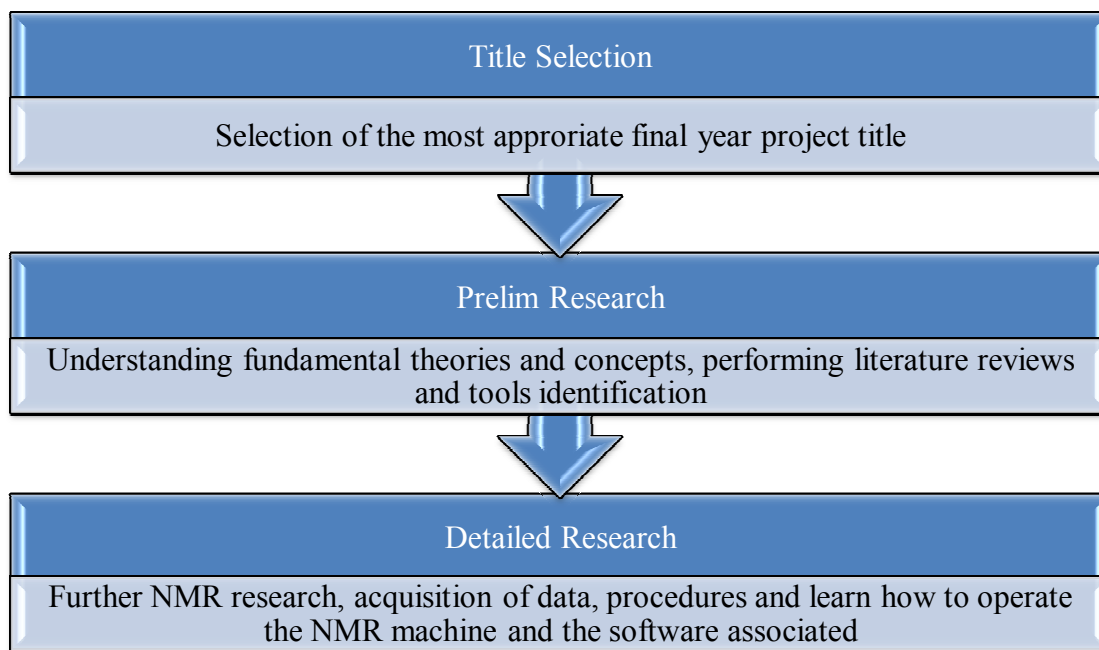


Figure 11: SDR Model

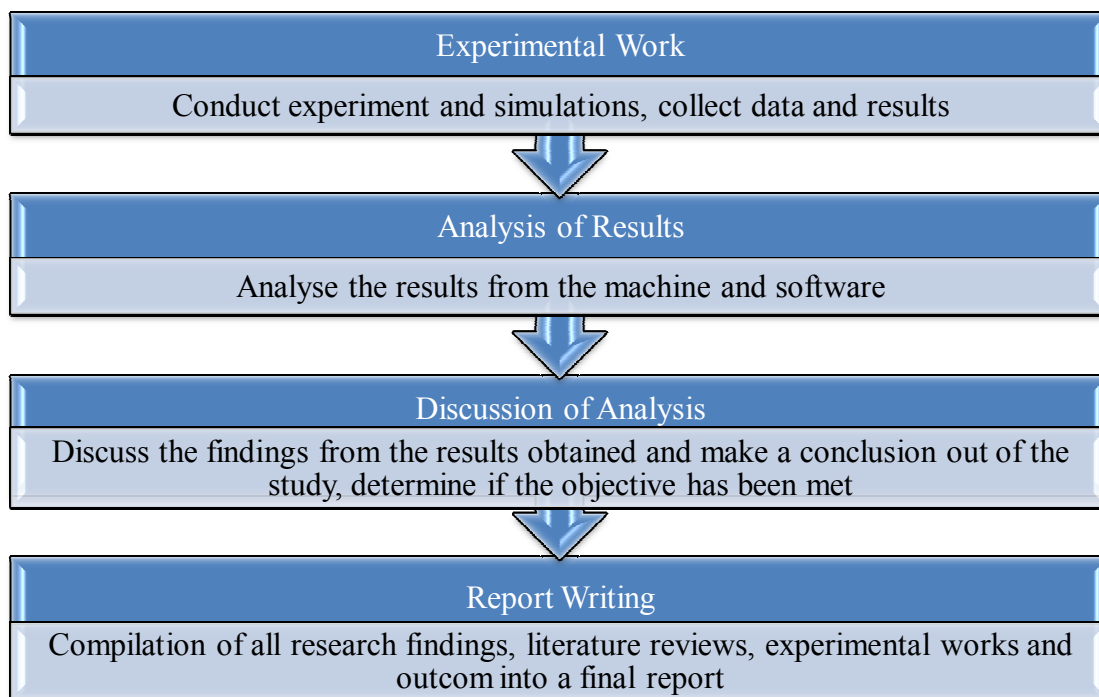
CHAPTER 3: METHODOLOGY

3.1 GENERAL RESEARCH METHODOLOGY

FYP 1:





For next semester's FYP 2, below is the planned workflow.



3.2 PROGRESSION CALENDER

OCTOBER 2011 (1) <ul style="list-style-type: none"> - FYP briefing - Topic Selection Objective: <ul style="list-style-type: none"> - Preliminary research on topics of choice, make a choice accordingly 	OCTOBER 2011 (2) <ul style="list-style-type: none"> - Reading background information about the area of study Objective: <ul style="list-style-type: none"> - Understand the basic theories, fundamentals and theories behind Nuclear Magnetic Resonance Studies 	NOVEMBER 2012 <ul style="list-style-type: none"> - Submission of extended proposal -Research study on NMR Objective: <ul style="list-style-type: none"> -To grasp more clearly the concepts of NMR - Create/edit/find algorithms for permeability predictions using NMR data
DISEMBER 2011 <ul style="list-style-type: none"> - Acquire core samples Objective: <ul style="list-style-type: none"> - Gather core samples to be used in lab experiments in determining permeability 	JANUARY 2012 <ul style="list-style-type: none"> - Samples could not be used, find ways to create own core from scratch Objective: <ul style="list-style-type: none"> Find a way to make a core with known parameters as this would lessen ambiguity and uncertainty of latter results 	FEBRUARY 2012 <ul style="list-style-type: none"> - Find ways to create own core from scratch (continued) - Create Core - Trip to PRSB to use NMR lab
MARCH 2012 <ul style="list-style-type: none"> - Prepare Progress report to be submitted to coordinator and supervisor - Send core to PRSB - Attend compulsory FYP 2 Seminar 	APRIL 2012 <ul style="list-style-type: none"> - Get results from PRSB - Analyse and discuss result - Come up with conclusion and suggestions for further studies 	MAY 2012 <ul style="list-style-type: none"> - Poster Exhibition - Oral presentation - *Submission of Project Dissertation <p>* This is the Dissertation. Upon submission, this has been completed</p>

LEGEND		Work Done
		Work To Do

3.3 GANTT CHART

Milestone for the Second Semester of 2-Semester Final Year Project –FYP1

No	Detail/ Week	1	2	3	4	5	6	7	8	9	10	11	12	13	14
1	Topic selection														
2	Preliminary literature review														
3	Submission of extended proposal														
4	Research study on NMR														
5	Acquire Samples														
6	Conduct lab experiment														
7	Proposal defence and progress evaluation														
8	Study results of the analysis														
9	Discussion on the project findings														
10	Analysis on project findings														
11	Submission of interim draft														
12	Submission of interim report														

	Suggested milestone
	Process

Milestone for the Second Semester of 2-Semester Final Year Project –FYP2

No	Detail/ Week	1	2	3	4	5	6	7	8	9	10	11	12	13	14
1	Project Work Continue														
2	Submission of Progress Report 1														
4	Submission of Progress Report 2														
5	Seminar (compulsory)														
7	Poster Exhibition														
8	Submission of Dissertation (soft bound)														
9	Oral Presentation														
10	Submission of Project Dissertation (Hard Bound)														

	Suggested milestone
	Process

3.4 CORE SAMPLE

3.4.1 Acquire Core Sample

Five core samples of known properties taken from PRSB warehouse

3.5 PERMEABILITY USING PERMEAMETER POROSITY METER (POROPERM)

3.5.1 Connections

1. Connect the POROPERM to the main power supply
2. Connect the air to the air inlet
3. Connect the Nitrogen or Helium (in this case, Helium) to gas inlet

3.5.2 Core Installation

1. Select core holder corresponding to the core diameter
2. Mount core holder with the sleeve
3. Install the core holder on its support and lock it
4. Select upper and lower plugs according to the diameter and screw it on the ram

3.5.3 Operating Mode

Sensor Calibration (Figure 12)

1. Select the “transducer calibration” tab
2. In the <<Config>>, select <<Auto>>, and 270 psi for P_{\max} , and 10 psi for ΔP (noted as DeltaP)
3. Install the standard volume $N^{\circ} > 1$
4. Confine
5. Connect the pressure calibrator at the outlet

6. Click on the <<Start Calib.>> button
7. Follow instructions
8. End

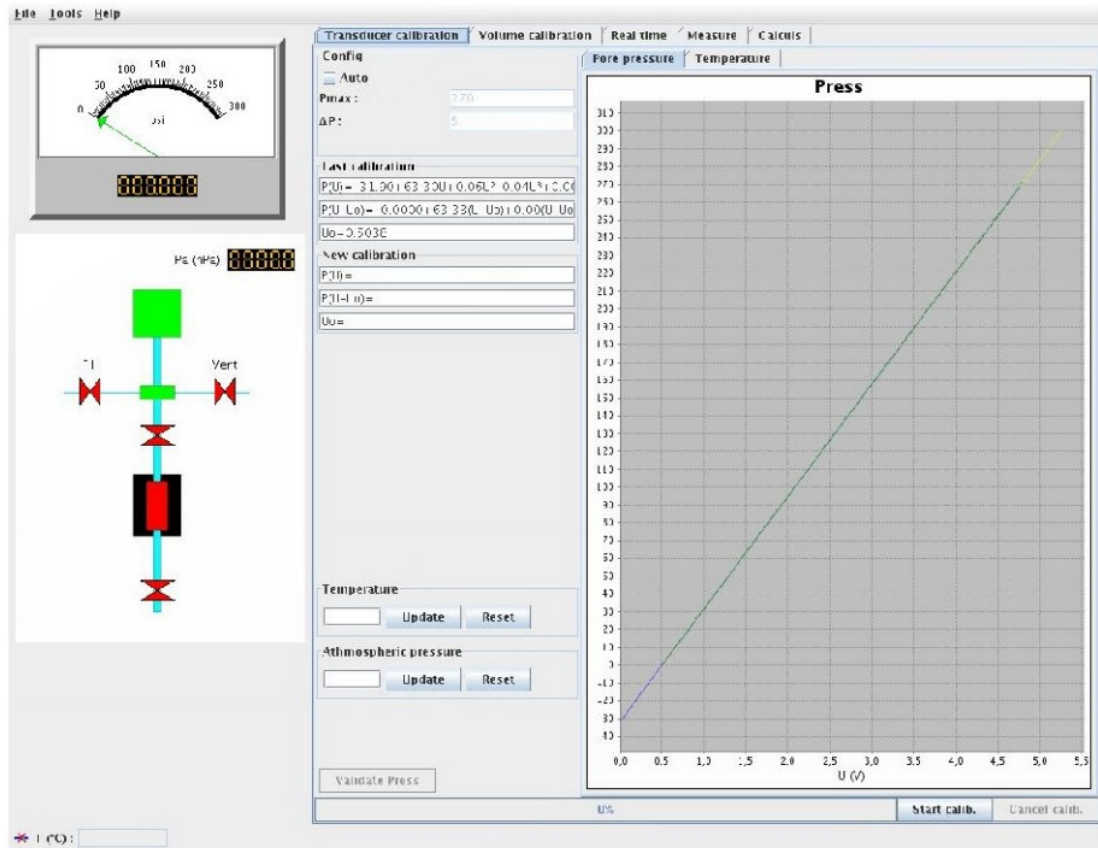


Figure 12: Sensor Calibration

Tank Volume Calibration (Figure 13 and Figure 14)

1. Click on the “Clear calib. Tank” button
2. Install the standard N^o2
3. Select in the table the line of N^o1
4. Confine
5. Click on the “Start Calib.” button. NOTE: after clicking, the button will be unavailable
6. Wait for the availability of the “Start Calib.” button.
7. Vent the confining
8. Replace the standard by the next one
9. Select the next line in the table
10. Repeat step 4-9

11. When the last standard is finished, click on “validate calib Tank” button
12. Obtain V_d , V_t and the correlation coefficient
13. Install standard N°1 (without hole)
14. Check porosity option
15. Confine
16. Click on the “Start” button. NOTE: after clicking, button will be unavailable
17. When measurement of porosity finish, find a negative number for the “ V_p (cc)” field (e.g.: -5.0), note down value.
18. Click the “Cancel” button
19. Input the absolute value in the “ V_{d0} ” field of the “Volume calibration panel” (e.g.: 5.0)

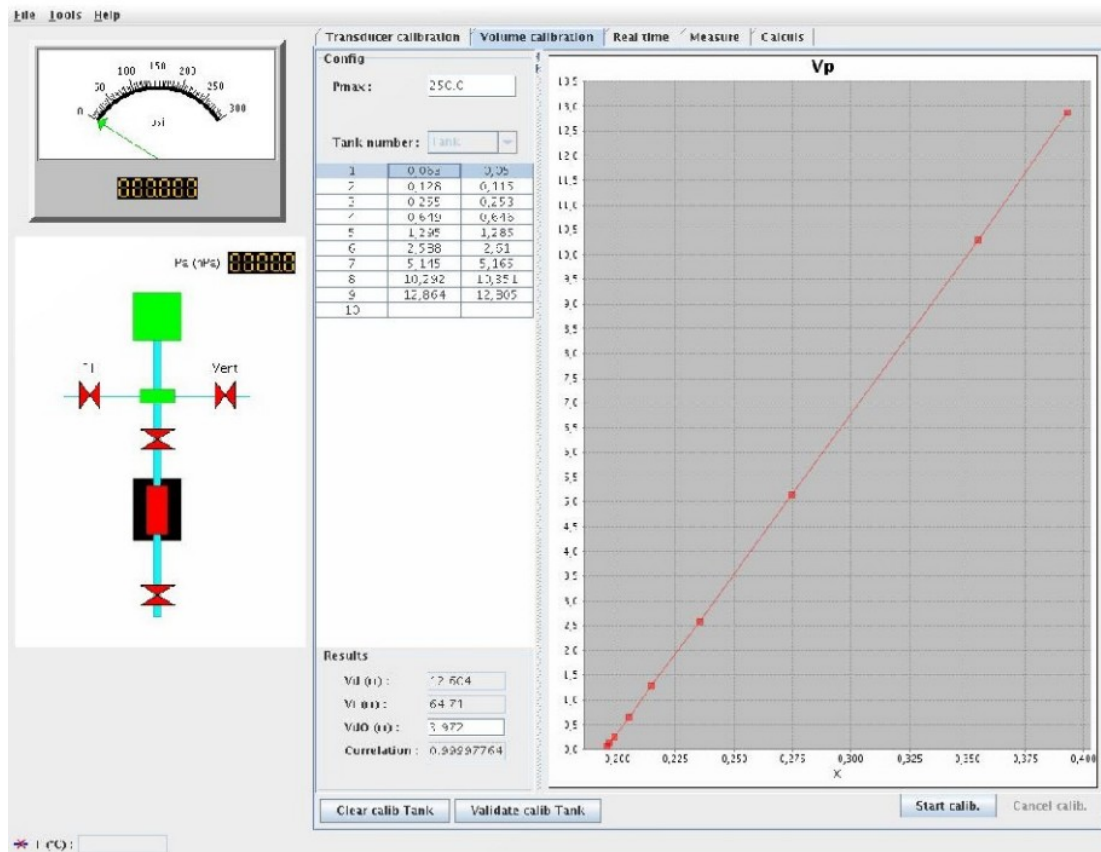


Figure 13: Tank Volume Calibration 1

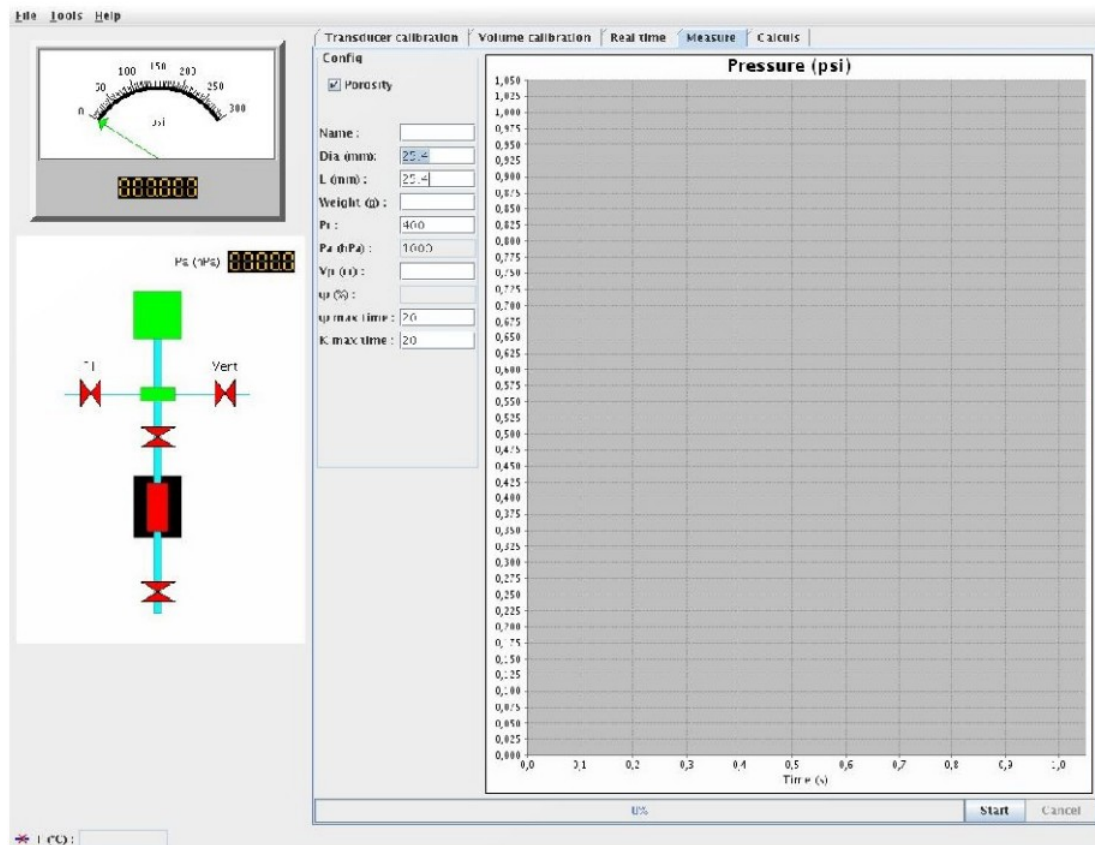
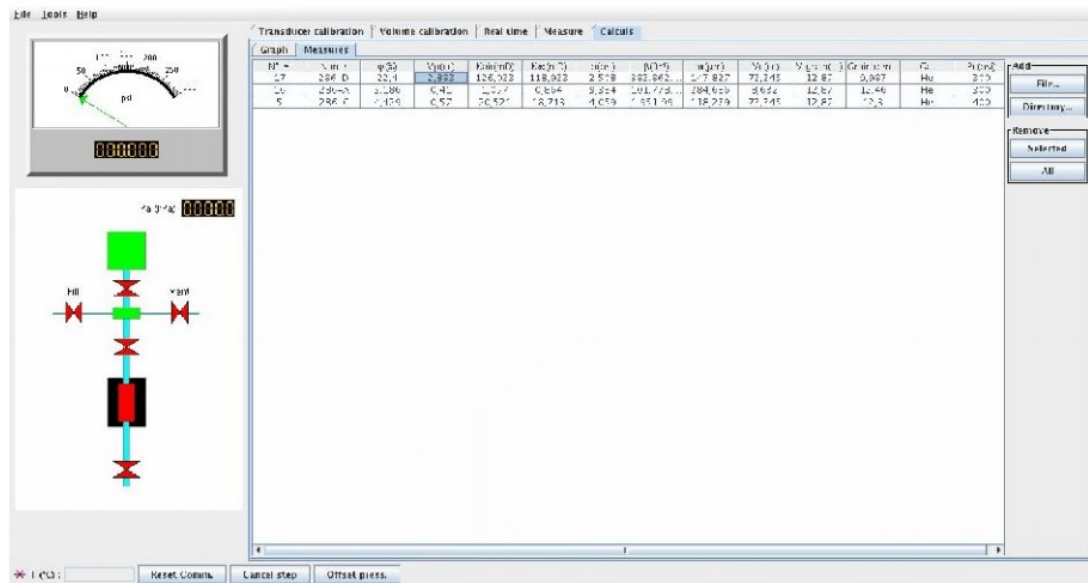


Figure 14: Tank Volume Calibration 2

Sample Measurement (Figure 15)

1. In the “measure” tab panel, fill in the fields which has “Name”, “Diameter(mm)”, “Length(mm)”, “Weight(g)”, and “Confining Pressure (psi)”
2. If the “Porosity” option is not checked, fill also the Pore volume (cc)
3. Choose the measurement needed for the sample (in this case, Porosity and Permeability as no option for permeability only)
4. Install the sample
5. Click on the “Start” button.
6. Wait for the measurements to finish
7. Go to “Calcul” tab and view results. Note results.



- l. Relaxation delay (us): RD: value: 2 seconds
- m. 90 – 180 degree pulse gap (us):TAU: value: 120
- n. 90 degree pulse phase list: PH1: value: 213
- o. Receiver phase list: PH2: value: 213
- p. 180 degree pulse phase list: PH3: value: 213
- q. Dummy Scan: DS: value: 0
- r. RF amplitude (%): RFA0: value: 100

5. Start the software for analysis
6. After T_2 curve has appeared, the T_2 cutoff is determined using Win DXP software
7. All results will be printed out and the experiment will be repeated with remaining cores
8. Analysis and discussion of the T_2 distribution is to be made to find the permeability of the sample

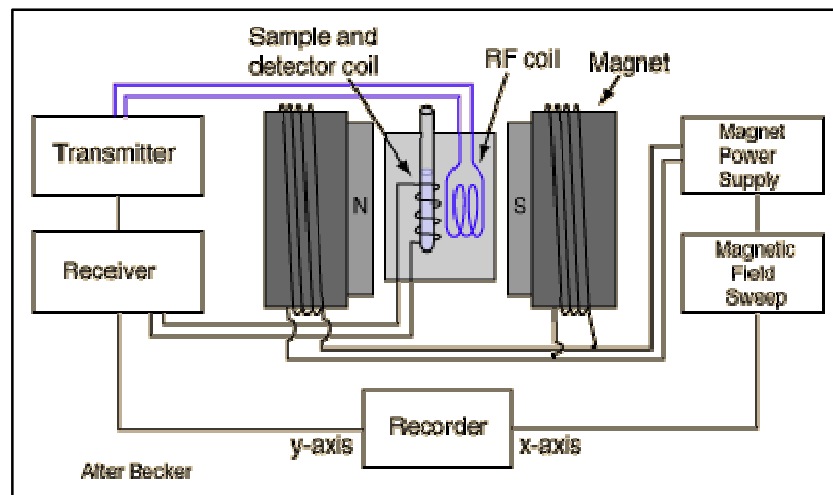


Figure 16: NMR Imaging Schematic Diagram



Figure 17: MARAN ULTRA Machine

3.7 METHOD OF ANALYSIS

1. Calculate the permeability using both Coates Model and SDR Model
2. Compare the permeability results between both models with the result from the lab, assuming the lab results are most accurate
3. Discuss the findings

CHAPTER 4: RESULTS AND DISCUSSION

4.1 DESCRIPTION OF NMR SPECTRA BY SAMPLE

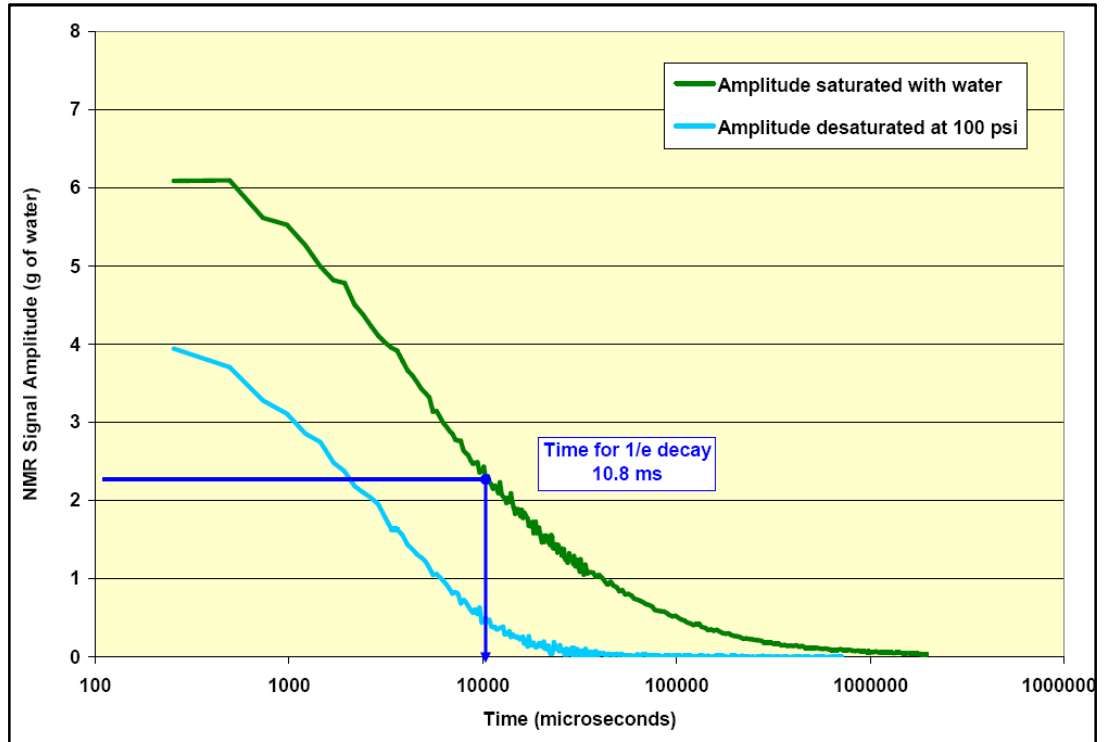


Figure 18: NMR T2 Relaxation Raw Data Sample #1

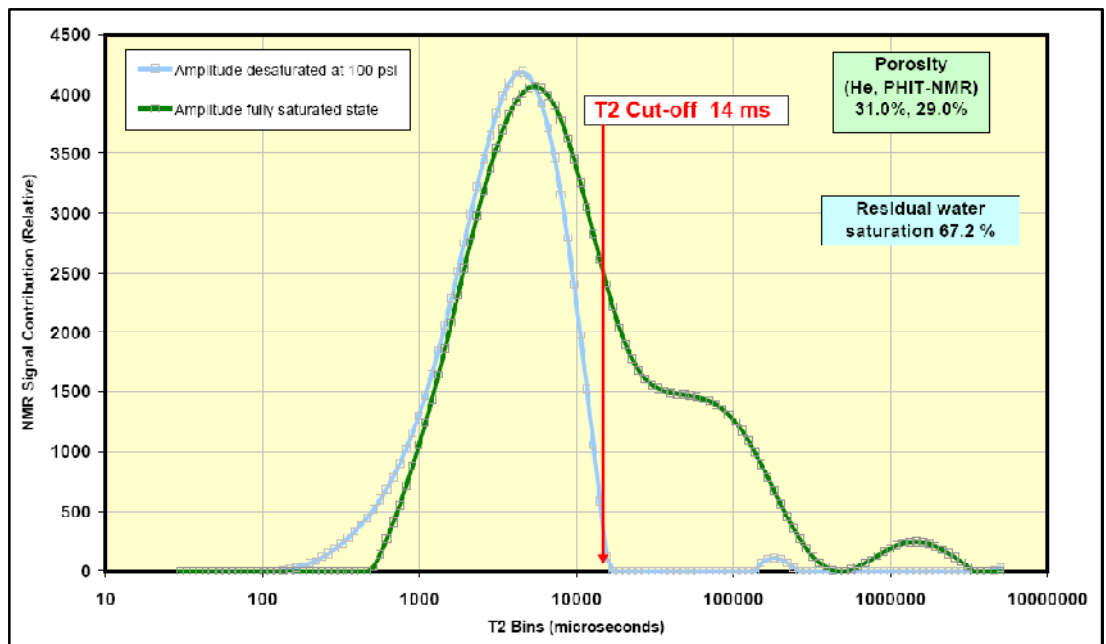


Figure 19: NMR T2 Relaxation Time Distributions Sample #1

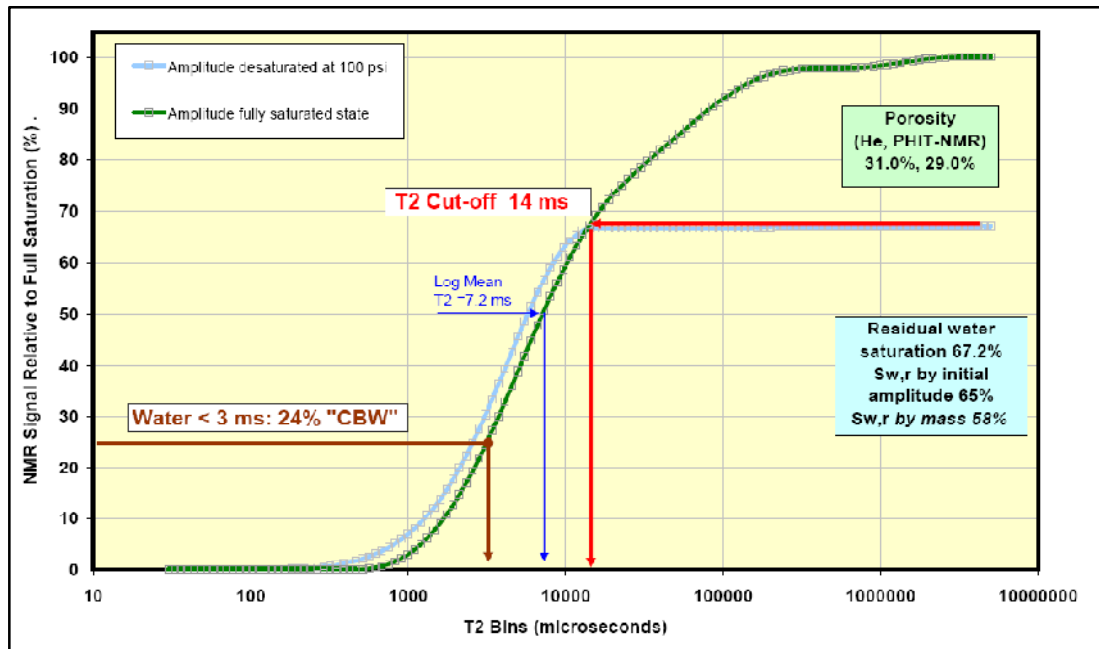


Figure 20: T2 Cumulative Relaxation Time Distributions Sample #1

Sample #1

Raw decay curve of the saturated sample is a fairly smooth sigmoid.

The saturated T_2 curve reflects distributed pore size distribution with a large number of small pores (3-20 milliseconds peak) and a decreasing population of larger pores represented by the shoulder of T_2 values around 100 milliseconds. A small T_2 bump at around 1 second probably came from trapped bulk water. This peak can be subtracted for volumetric calculations. In this sample, log mean T_2 is half of the sum- T_2 cut-off value, which is lower than the “default” values cited for sandstones (14 milliseconds) but very clearly defined. The residual saturations based on initial amplitude and mass are respectively smaller by 2.2% and 8.8 % than the sum- T_2 cut-off. This is a typical result, produced by the data inversion procedure. The “clay bound water” determined from the < 3 milliseconds criterion amounts to 24% of total water (7 pu).

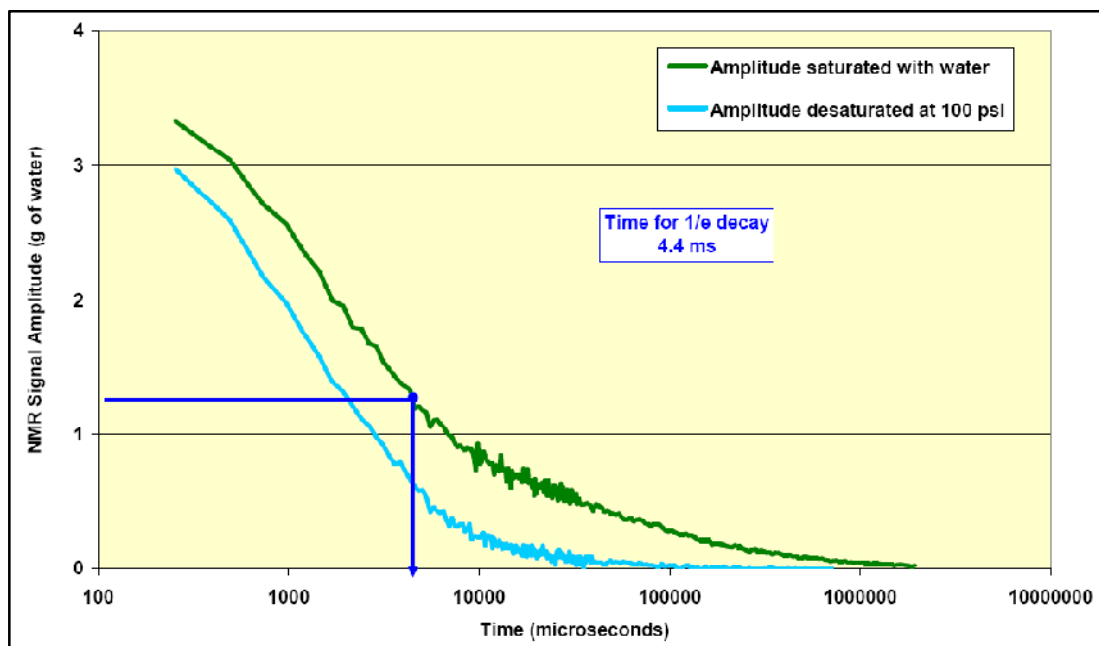


Figure 21: NMR T2 Relaxation Raw Data Sample #2

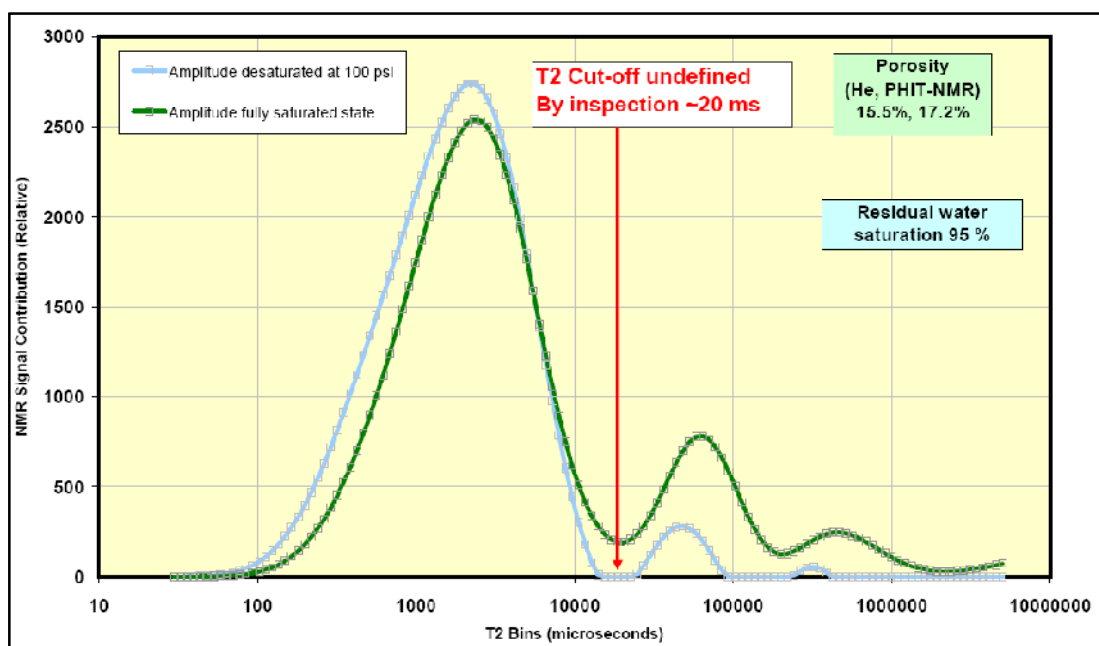


Figure 22: NMR T2 Relaxation Time Distributions Sample #2

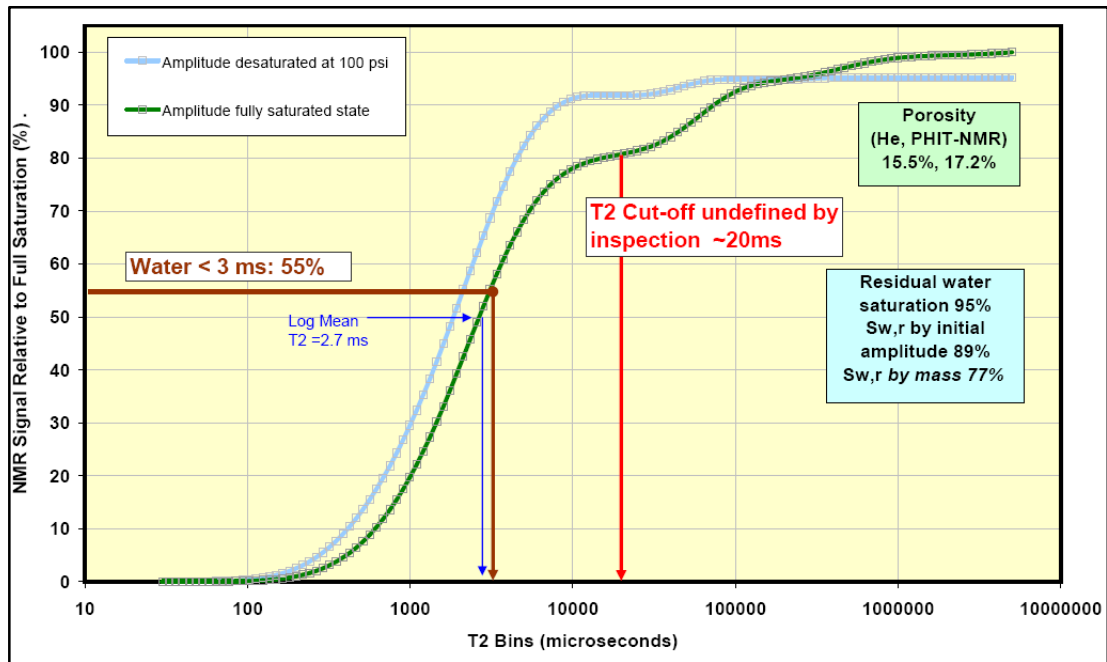


Figure 23: T2 Cumulative Relaxation Time Distributions Sample #2

Sample #2

Raw decay curve of the saturated sample is a stretched sigmoid with a long tail. The saturated T_2 distribution is bimodal.

It is dominated by short T_2 values (small pores and bound water); with a subsidiary peak around 70 milliseconds. The desaturated sample data shows a single peak roughly coincident with the short T_2 data and with a small bump at around 50 milliseconds (this region, 50-70 milliseconds, is partly free water, but partly trapped, showing that some large pores are inaccessible through small throats). The small fraction of moveable water is distributed over a broad size range. The cut-off value is undefined by the conventional method, but by inspection of the curves, a value of around 20 milliseconds looks to be plausible. The large amount of water < 3 milliseconds, about 55-60% of total NMR detected water, is actually capillary trapped for the most part, rather than truly being clay bound, since the majority of residual water mass is lost following non-aggressive drying at 46 °C.

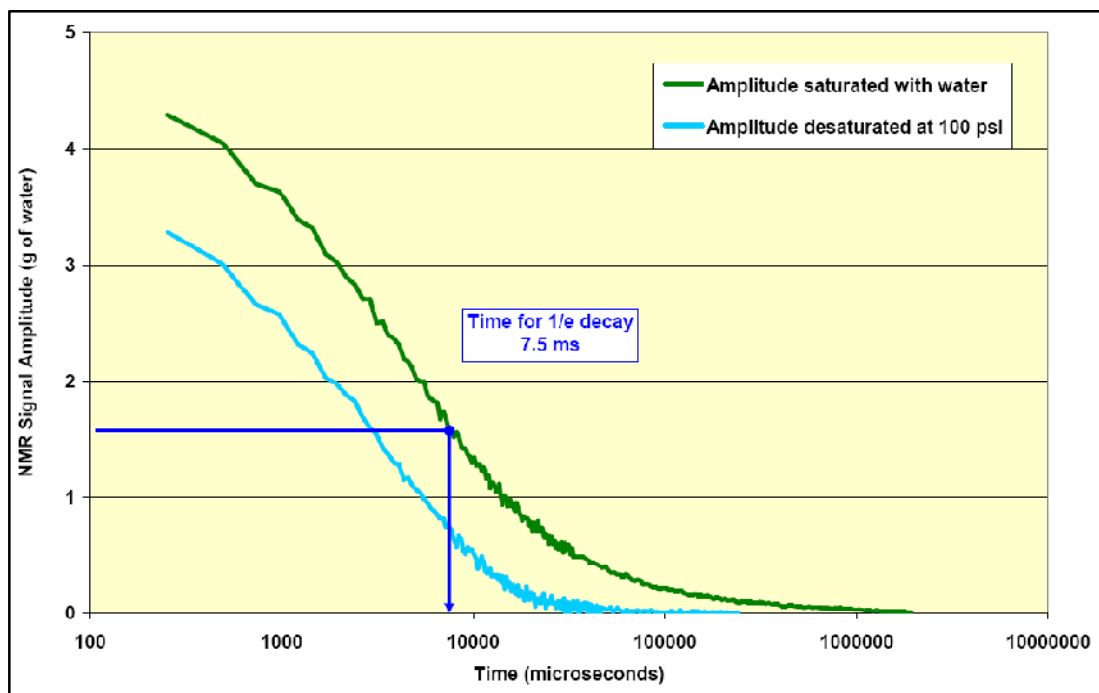


Figure 24: NMR T2 Relaxation Raw Data Sample #3

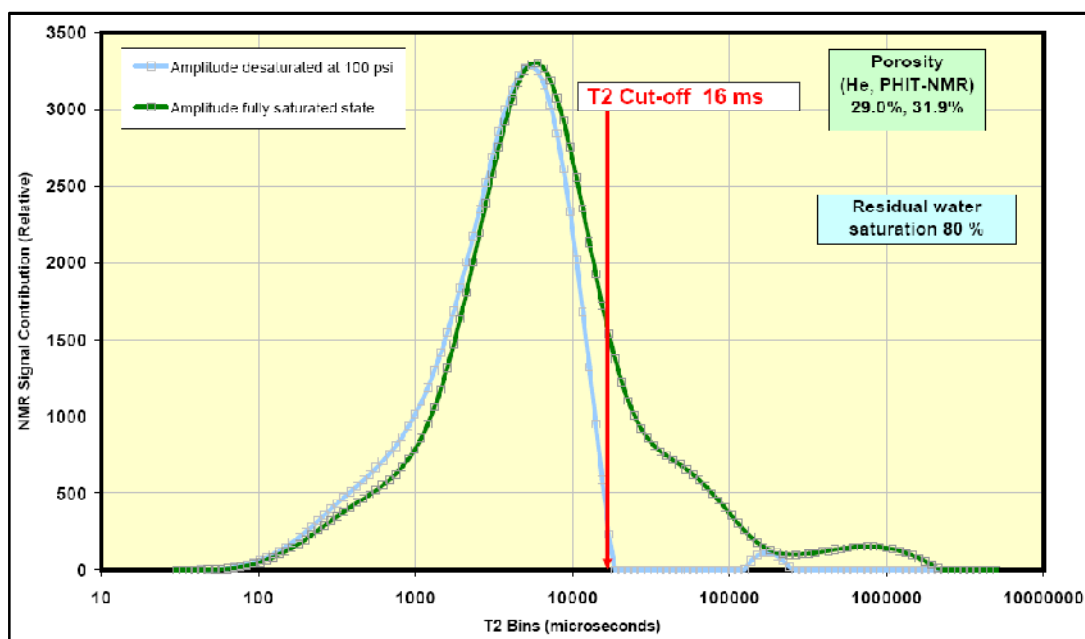


Figure 25: NMR T2 Relaxation Time Distributions Sample #3

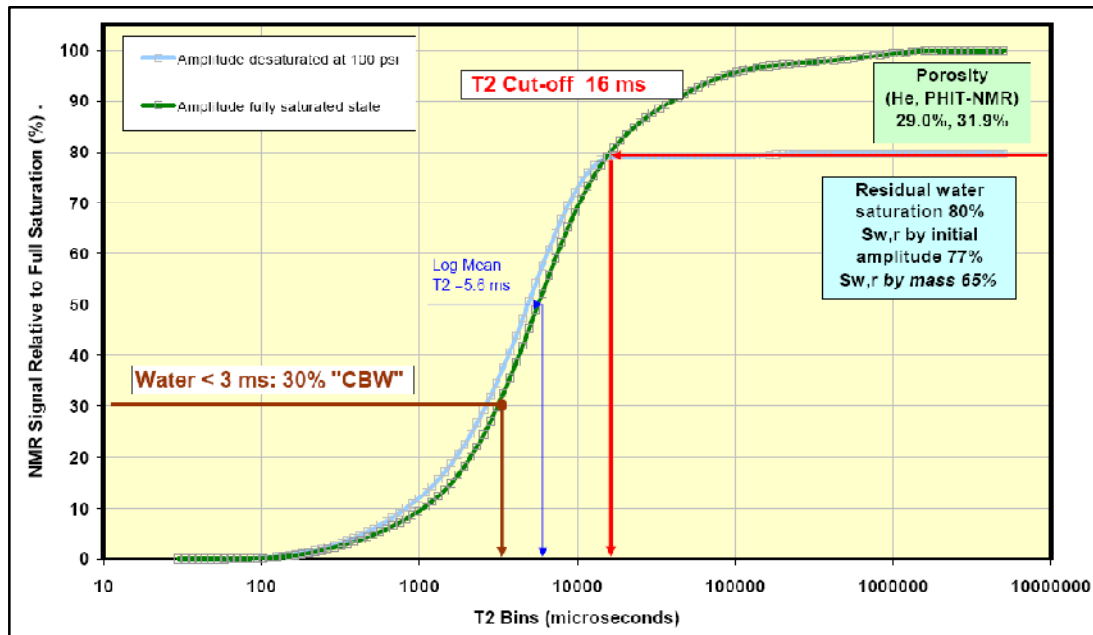


Figure 26: T2 Cumulative Relaxation Time Distributions Sample #3

Sample #3

Raw decay curve of the saturated sample is a fairly smooth sigmoid with a steep middle section.

The saturated T_2 curve shows an unusual shape with a distinct peak at 7-8 milliseconds but tapering both sides. The amount of water relaxing at times less than 5 milliseconds is rather small, suggesting that clay bound water is less important than trapped capillary water in fine pores (30% of the water is less than 3 milliseconds). Additionally, there is a subsidiary region of longer T_2 extending to 3 seconds, which in part most likely an indication of some larger pore space. The residual saturation is very high, but one would expect that at higher capillary pressure this water could be moved. The cut-off is rather short (16 milliseconds), about half the “default” value for clastics. Note that the cut-off is at longer T_2 than the main peak, which explains this high saturation of trapped water at 100 psi capillary pressure.

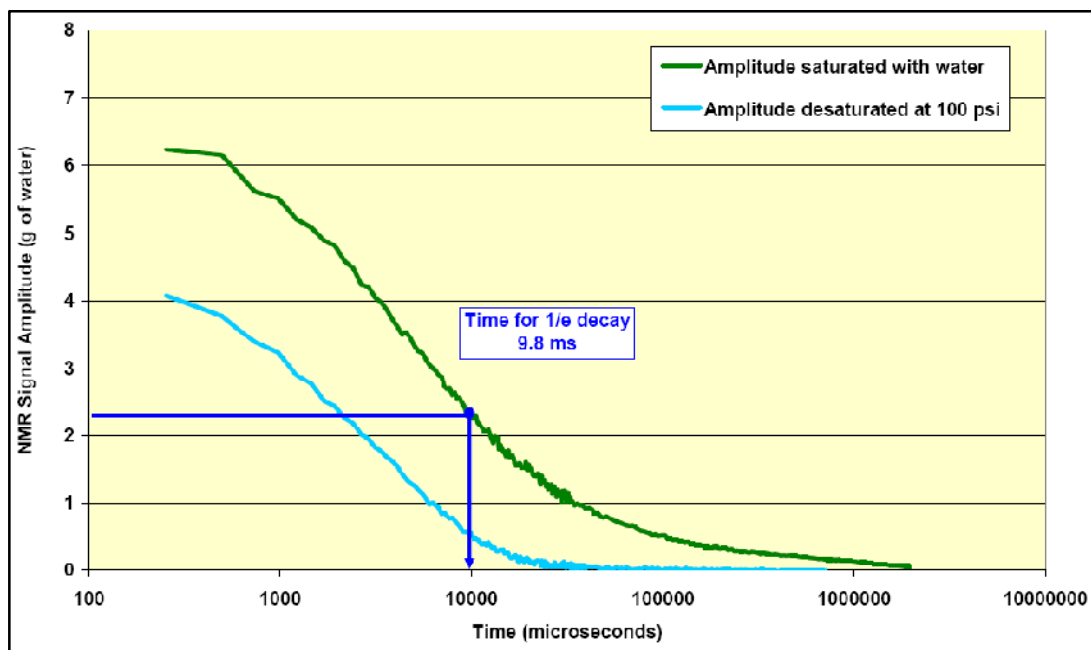


Figure 27: NMR T2 Relaxation Raw Data Sample #4

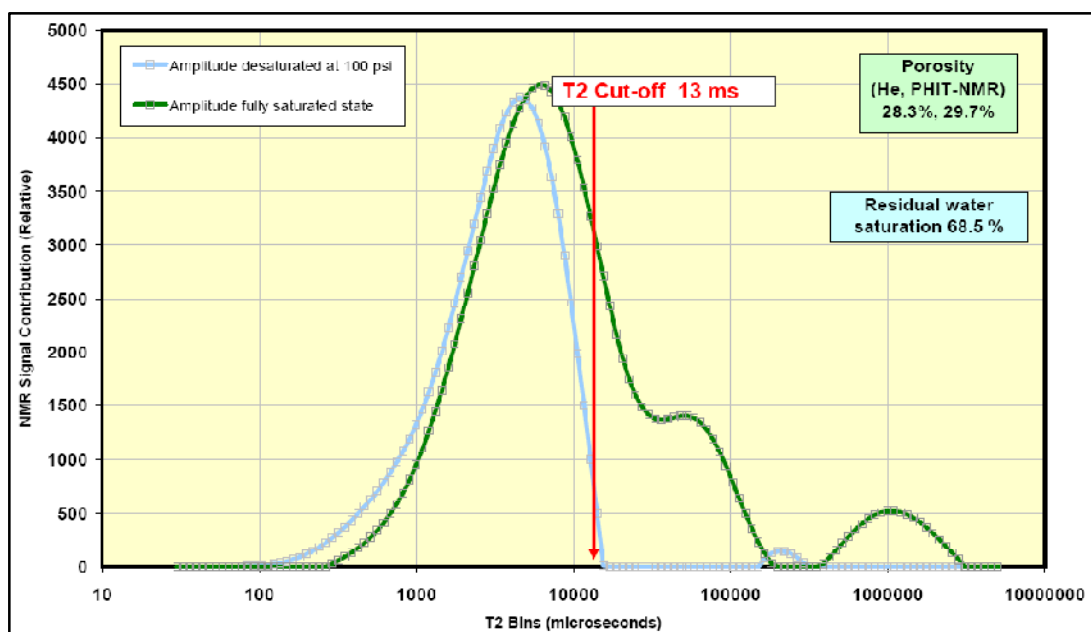


Figure 28: NMR T2 Relaxation Time Distributions Sample #4

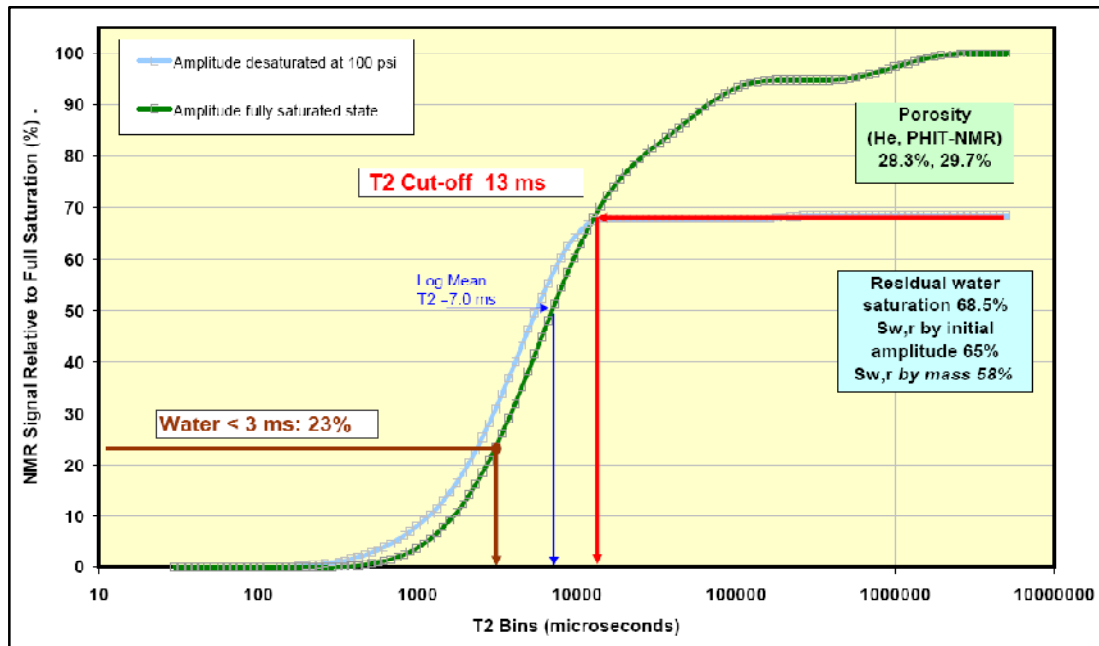


Figure 29: T2 Cumulative Relaxation Time Distributions Sample #4

Sample #4

The raw decay curve shows a very gentle sigmoidal shape, with a tail to longer times.

The T_2 curve for the saturated sample has a main peak at about 7-8 seconds. The peak centred on around 1 second is most likely water trapped and can be ignored for processing. The shoulder peak at around 70-100 milliseconds is significant, because it represents at least some large pores; however, given the low permeability we can infer that these are only connected via smaller pores, so the overall porosity is not efficiently used. High (over 65%) residual water values from Sum T_2 and initial amplitude methods agree well for this sample, and typically both are larger than the mass-based residual water value of 58%. The conventional graphical projection method on the cumulative curve gives a cut-off for free water of 13 milliseconds, which is rather low but not surprising for this sample set. The amount of clay bound water indicated is small. The < 3 milliseconds criterion, which we know is a gross overestimate for these samples, gives about 22-23% or 7 pu.

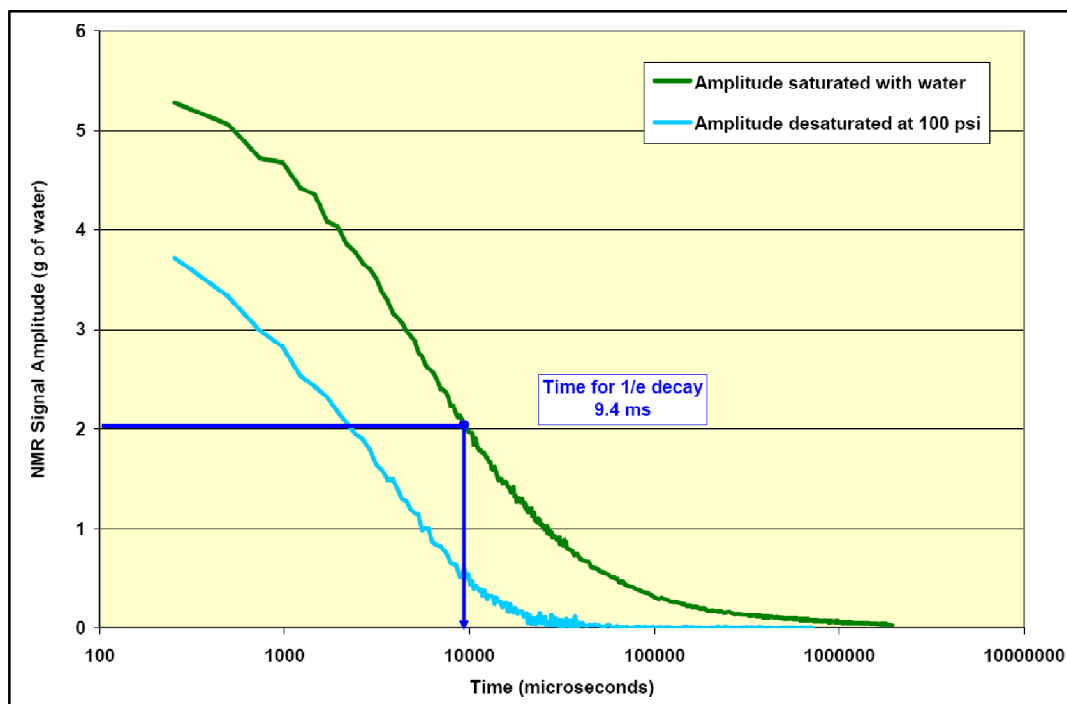


Figure 30: NMR T2 Relaxation Raw Data Sample #5

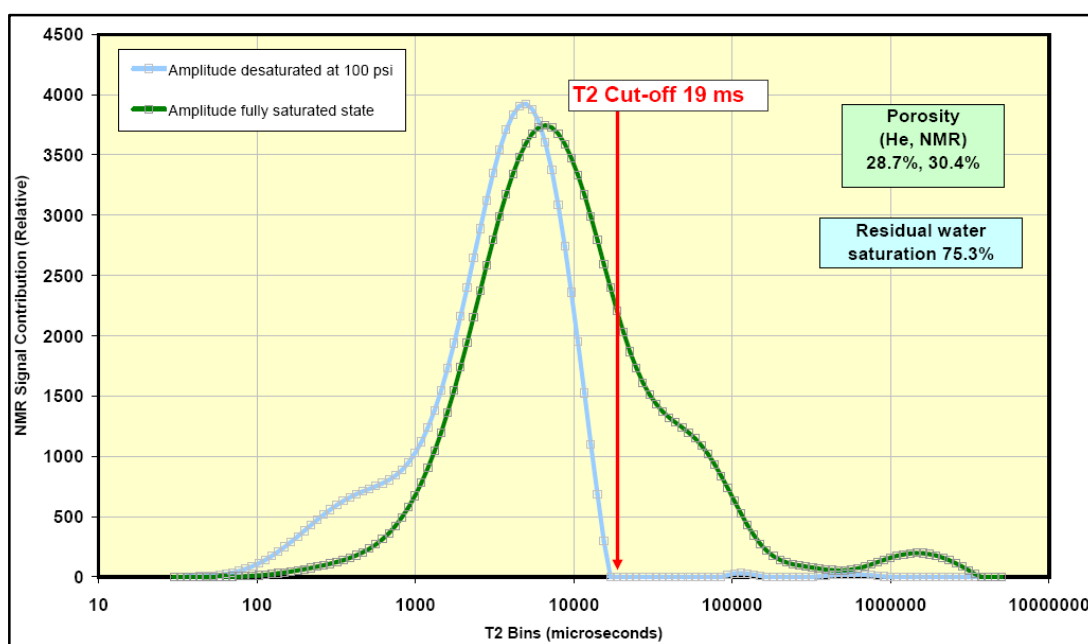


Figure 31: NMR T2 Relaxation Time Distributions Sample #5

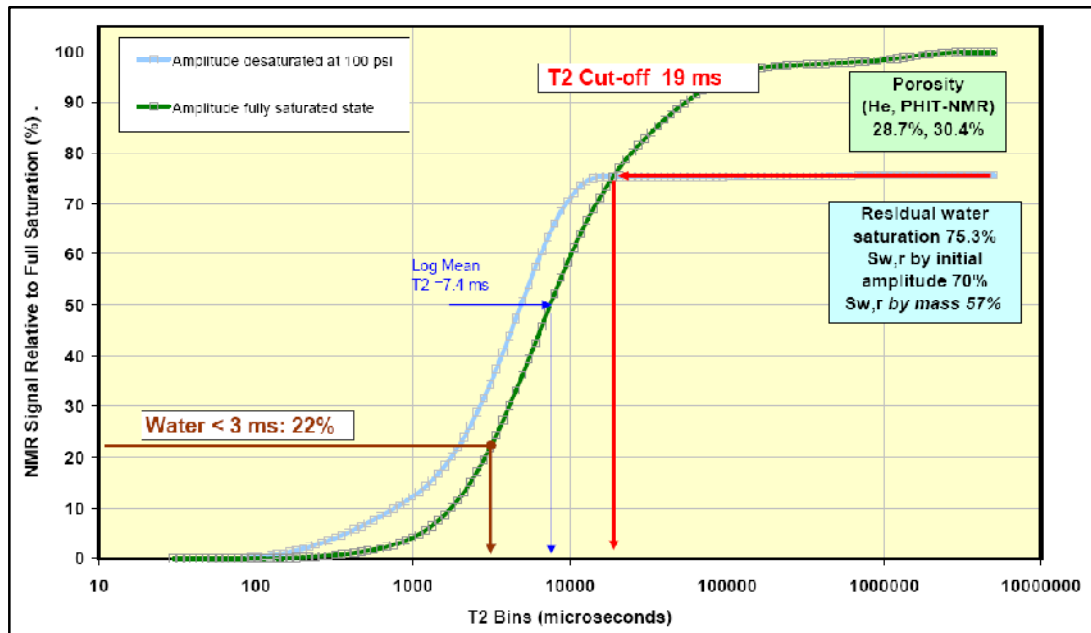


Figure 32: T2 Cumulative Relaxation Time Distributions Sample #5

Sample #5

The raw decay curve is a sigmoid with steep middle section, and small tail.

From this and the inverted saturated T_2 distribution we can infer the dominance of small pores with the peak coincident with the log mean relaxation time (7-8 milliseconds T_2). There is a small shoulder region extending to much longer T_2 , which represents the larger pores. The permeability of this sample is about twice that of Sample #4, so we can infer that these larger pores are somewhat better connected even though the preponderant T_2 values are similar and the porosity is identical. The cut-off of 19 milliseconds comes after the main T_2 peak but before these smaller pores. The relaxation times of the trapped unsaturated sample are shorter than for the corresponding part of the saturated T_2 curve. The amount of clay bound water is, as in the other samples, much smaller than trapped capillary and film water

4.2 PERMEABILITY PREDICTION

4.2.1 Coates Model

$$k = \left[\left(\frac{\Phi}{C} \right)^m \left(\frac{FFI}{BVI} \right)^n \right]$$

Where:

k = permeability

ϕ = porosity

C = formation dependent coefficient, 0.096

FFI = Free Fluid Index (Volume of Movable Free Fluid) where $FFI = \phi - BVI$

BVI = Irreducible Bulk Volume (obtained through Cutoff BVI or Spectral BVI)

m = assumed to be 2

n = assumed to be 2

Sample	NMR Porosity (%)	T2 Cutoff (ms)	BVI (%)	FFI (%)	Helium Permeability (md)	Coates Permeability (md)
Sample #1	29.0	14	9.163	19.837	23.4	42.8
Sample #2	17.2	20	10.729	6.471	1.3	1.2
Sample #3	31.9	16	12.676	19.224	4.52	25.4
Sample #4	29.7	13	8.761	20.939	8.61	54.7
Sample #5	30.4	19	7.990	22.41	17.6	78.9

4.2.2 SDR Model

$$k = a T_{2lm}^2 \phi^4$$

Where

k = permeability

a = formation dependant coefficient

T_{2lm} = logarithmic mean of T_2 distribution

ϕ = effective porosity

Sample	Helium Porosity	T_{2lm} (ms)	1/e (ms)	Helium Permeability (md)	SDR Permeability (md)
Sample #1	0.310	7.2	10.8	23.4	26.9
Sample #2	0.155	2.7	4.4	1.3	0.3
Sample #3	0.290	5.6	7.5	4.52	9.9
Sample #4	0.283	7.0	9.8	8.61	15.4
Sample #5	0.287	7.4	9.4	17.6	14.9

The SDR permeability estimate, based on log mean T_2 does not work as well for this sample set, with squared error in log of permeability about 0.33. The calculation of permeability using the SDR equation but substituting the time value to decay to 1/e of the initial amplitude is intermediate in the absolute error, and predicts the same trends as observed.

4.3 OVERALL ANALYSIS

NMR amplitude itself is actually a very small source of error compared with other sources in the NMR petrophysical workflow. However it is likely to be less than 1%.

Unfortunately, significant errors might have arisen in the preparation of the samples such as the shape irregularity conformance and handling where wrapping and the saturations might become an issue. Especially discrepancies in mass balance which are largely due to wrong assumptions made, such as the assumption made that the detection of water in the initial amplitude is coming from a clean sample and is fully saturated, though the sample is prepared in lab as well and not taken from any site. Besides, the core was taken from the PRSB warehouse which might also contribute to a significant amount of error towards the readings due to weathering.

Uncertainties are inevitably associated with inverted data, which uses an arbitrary regularization parameter and imperfect mathematical model to convert the measured amplitude decay time series into relaxation time distribution. This is not only non-unique but also can have a significant bias, especially if the relaxation times are predominantly short. The signal to noise might be enormously higher in the lab than in the field, so the inversion of the lab data is robust, whereas the inversion and derived parameters from the field data will be questionable in most cases.

Compared with downhole data, the NMR data in this study differ in other ways too, namely;

- i. On one hand, there is a different prevailing temperature and pressure. Overburden pressure will reduce total porosity and in general, reduce T_2 , and stress will especially reduce the number of small, high aspect ratio pores which are more compliant.
- ii. On the other hand, the fluid viscosity is decreased at high temperature, making T_2 slightly higher for a given fluid, so, the effects are partly cancelled.
- iii. The sample volume in the lab is small, representing only one lithofacies, whereas in the field, the NMR sensitive volume in especially laminated shaly sequences will probably average shaly and sandier portions of the formation.

- iv. In the lab, the magnetic field is extremely homogeneous, so the T_2 can be measured reliably. In the downhole environment, the tool inevitably will face a field gradient in the sensitive zones, and this reduces the values of the measured T_2 to a certain extent. Again, this effect can be investigated with more detailed studies using applied field gradients.

The techniques used have demonstrated to hold good promise for prediction of reservoir properties, to be more specific, the permeability. However, there are still lots that could be done to improve the data accuracy and reliability. This includes but not limited to;

- i. More NMR lab measurements
- ii. Dielectric Log measurements
- iii. Vertical and horizontal resistivity measurements
- iv. This section analysis
- v. More rigorous resistivity modelling

CHAPTER 5: CONCLUSION AND RECOMMENDATION

5.1 CONCLUSION

In order to ensure that reservoirs are properly characterized, the integration of log and core measured data has to be done. Using only NMR will not suffice to predict permeability. The objective is to perform a thorough study of permeability based on the techniques described earlier in the report and thus the reason of no other outside integration. However it would be more helpful for the industry to integrate the log and core evaluations.

Accordingly, the fitting of parameters for the SDR model for permeability prediction produces a significantly accurate result if we assume the POROPerm reading is nearest to the true value while the Coates model generally shows a considerably high permeability prediction.

As a consequence of the generally very short T_2 values from the samples, the determination of clay bound water becomes critical. This could be done successfully using measurements on an air dried sample after completion of the other analysis. This extra measurement shows that the clay bound water defined on the basis of a 3 millisecond cutoff actually, includes for the most part, the trapped water which is lost by non aggressive drying.

The actual clay bound water could be determined by drying the samples at different relative humidity values and measuring the change in of the received signal. On this basis, drying at ambient conditions which is around 22°C to 28°C and also with relative humidity of 45% to 55% could remove all capillary water, leaving a certain number of water layers adhering to the internal surface of the rock which most probably is dominantly of clay bound fluid.

The change in sample mass from this stage of drying to a more aggressive oven would show whether the change will be relatively small (it is projected to be small),

which would then indicate that the water associated to clays is quite tightly bound, thermodynamically speaking, and may represent a molecular monolayer.

The remaining discrepancies in weight and signal size in the vacuum dried samples are thought to be due to residual traces of hydrocarbons in the rock.

5.2 RECOMMENDATION

- 1. Permeability predictions should include other non-conventional models even though they might be more complex, these non-conventional models include but not limited to:**
 - a. HSCM model, developed by Hidajat et al. (2002)**
 - b. Kozeny-Carmen Model (Kozeny, 1927; Carman, 1937; 1938; 1956)**
 - c. The Swanson model (1981)**
 - d. The Breg Model (Breg, 1970) or The Breg Model (simplified by Breg, 1975)**
 - e. The Van Baaren Model (Van Baaren.1979)**
 - f. RGPZ model (unpublished discussion paper by André Revil, Paul Glover, Phillippe Pezard, and M. Zamora)**
2. It seems likely that a substantial amount of clay bound water measured by NMR at T_2 less than 3 milliseconds is actually associated with surface film water and not actually clay minerals. This could further be studied. Previous findings which says 3 milliseconds and below should be clay bound water is not necessary correct, not also am I saying it is wrong, but this inference must be used with caution and future studies could be made on this subject matter.
3. The cut offs in T_2 between capillary and free water are extremely short. More research would be needed to discover why this is the case.
4. NMR analysis conducted without specific reference to microstructure can sometimes give misleading interpretations. Therefore, microscopic analysis would be recommended to understand more details of the pore structures and their relation to mineralogy, cement, microfacies and other properties.

5. NMR tools run at short echo spacing and long wait times would produce very useful results. With long wait times, T_2 cutoffs and mean T_2 would be easier to predict and have a better accuracy
6. Non aggressive sample preparation can leave traces of impurities in the rock. These residues can be studied and quantified to tell us more about the wettability and other properties.
7. Permeability prediction should be carried out with multiphase fluids as the real reservoir might not only have one phase. Thus, a true or near true estimate could be done and a stronger correction factor could be produced.

ABBREVIATIONS AND NOMENCLATURES

a	=	formation dependant coefficient
C	=	formation dependent coefficient
D	=	diffusion constant
D_a	=	apparent diffusion coefficient of pore fluid
D_w	=	apparent diffusion coefficient of water
FFI	=	Free Fluid Volume
FID	=	Free Induction Decay
BVI	=	Irreducible Bulk Volume (obtained through C_{utoff} BVI or Spectral BVI)
G	=	magnetic field gradient
HI	=	Hydrogen index
k	=	permeability
MFFI	=	Volume of free fluids or movable fluids
$M_i(0)$	=	initial magnetization from i^{th} component of relaxation
$M_{100\%}(0)$	=	amplitude of CPMG echo train at time zero obtained from MRIL water-tank calibration (100% porosity)
t	=	elapsed time
T_1	=	NMR longitudinal relaxation time constant
T_2	=	NMR transverse relaxation time constant
$T_{2\text{int}}$	=	intrinsic T_2 of the pore fluid ($1/T_{2\text{int}} = 1/T_{2\text{bulk}} + 1/T_{2\text{surface}}$)
γ	=	gyro magnetic ratio for hydrogen
ϕ	=	porosity (obtained from MPHI by Time Domain Analysis model or Diffusion Analysis model)
$T_{2\text{lm}}$	=	logarithmic mean of T_2 distribution
$\Delta\phi$	=	difference in hydrocarbon filled porosity obtained from the difference of the two echo trains
ϕ^*_{fluids}	=	apparent fluids filled porosity obtained from the difference of the two echo trains

REFERENCES

1. NMR Logging Principles & Applications by George R. Coates, Lizhi Xiao, and Manfred G. Prammer
2. Nuclear Magnetic Resonance Imaging – Technology of the 21st century by Kenyon, Kleinberg, Straley, Gubelin, and Morriss
3. Borehole Geophysics, Nuclear Magnetic Resonance (NMR) Logging by Professor Michael Riedel
4. Brownstein, K.R., and Tarr, C.E., 1979, Importance of Classical Diffusion in NMR Studies of Water in Biological Cells, Physical Review, Series A, V. 19
5. Sandor, R.K.J., and Looyestijn, W.J., 1995, NMR Logging - The New Measurement, Shell International Petroleum Maatschappij, The Hague, The Netherlands
6. Prammer, M.G., et al., 1996, Measurements of Clay-Bound Water and Total Porosity by Magnetic Resonance Logging, SPE 36522, 1996 SPE Annual Technical Conference and Exhibition Proceedings, v. Ω (Formation evaluation and reservoir geology)
7. Marschall, D., 1997, Magnetic Resonance Technology and its Applications in The Oil and Gas Industry, Part 2, Petroleum Engineer International, v. 70, no. 4)
8. Earth & Planetary Sciences, Lecture EPS-550, Professor Michael Riedel, Winter 2008
9. Ahmed, U., Crary, S.F., and Coates, G.R., 1989, Permeability Estimation; The Various Sources and Their Interrelationship, SPE 19604, 1989 SPE Annual Technical Conference and Exhibition Proceedings, v. Ω (Formation Evaluation and Reservoir Geology)
10. Marschall, D., Gardner, J., and Curby, F.M., 1997, NMR Laboratory Measurements - Requirements to Assure Successful Measurements That Will Enhance MRI Log Interpretation, Paper SCA 9704
11. Akkurt, R., Moore, A., and Freeman, J., 1997, Impact of NMR in The Development of a Deepwater Turbidite Field, Paper SS, in 38th Annual SPWLA Logging Symposium Transactions

12. Mardon, D., et al., 1996, Experimental study of diffusion and relaxation of oil-water mixtures in model porous media, paper K, 37th Annual SPWLA Logging Symposium transactions
13. Mardon, D., Prammer, M.G., and Coates, G.R., 1996, Characterization of light hydrocarbon reservoirs by gradient-NMR well logging, Magnetic Resonance Imaging, v. 14, nos. 7 and 8
14. Christian Straley, Dan Rossini (Schlumberger-Doll Research Centre), Harold Vinegar, Pierre Tutunjian (Shell Development Co.), Chris Morris (Schlumberger Wireline and Testing), Core Analysis by Low Field NMR, Paper SCA 9404
15. David Allen et al, 2000, Trends in NMR logging.
16. Matteson, A., Tomanic, J. P., Herron, M. M., Allen, D. F., and Kenyon, W. E., 1998, NMR relaxation of clay-brine mixtures, SPE-49008, in 1998 SPE Annual Technical Conference and Exhibition Proceedings, v. omega, Formation evaluation and reservoir geology: Society of Petroleum Engineers, p. 205–212.
17. Chitale, D.V., Gardner, J., and Sigal, R., 2000, Significance of NMR T2 distributions from hydrated montmorillonites, paper X, in 41st Annual Logging Symposium Transactions: Society of Professional Well Log Analysts, 10 p.
18. Straley, C., Rossini, D., Vinegar, H., Tutunjian, P., and Morriss, C., 1994, Core Analysis by Low Field NMR, Paper SCA-9404, In SCA International Symposium Proceedings: Society of Professional Well Log Analysts, Society of Core Analysts, Chapter At Large, P. 43–56.
19. Straley, C. et al.: “Core Analysis by Low Field NMR,” Paper SCA-9404 Presented At the 1994 Intl. Symposium of the Soc. Of Core Analysts, Stavanger (1994)
20. Prammer, M.G. et al.: “Measurements of Clay-Bound Water and Total Porosity by Magnetic Resonance,” The Log Analyst (November–December 1996) 37, No. 6, 61.
21. A. Matteson, J.P. Tomanic, M.M. Herron, SPE, D.F. Allen, And W.E. Kenyon, SPE, Schlumberger-Doll Research. “NMR Relaxation Of Clay/Brine Mixtures”, SPE Reservoir Evaluation And Engineering, Vol. 3, No. 5, October 2000
22. Matthias Appel.: “Nuclear Magnetic Resonance And Formation Porosity”, PETROPHYSICS, Vol. 45, No.3 (May-June 2004); P. 296-307; 5 Figures
23. Carr HY And Purcell EM: “Effects Of Diffusion On Free Precession In Nuclear Magnetic Resonance Experiments”, Physical Review 94, No. 3, (1954):630-638

24. Meiboom S And Gill D: “Modified Spin Echo Method For Measuring Nuclear Relaxation Times”, The Review Of Scientific Instruments 29, No. 8 (1958):688-691
25. Flaum C, Guru U And Bannerjee S: “Saturation Estimation From Magnetic Resonance Measurements In Carbonates”, Transactions Of The SPWLA 41st Annual Logging Symposium, Dallas, Texas, USA, June 4-7, 2000 Paper HHH
26. Timur, A., 1967, Pulsed Nuclear Magnetic Resonance Studies of Porosity, Movable Fluid and Permeability of Sandstones, SPE 2045, 42nd Annual Meeting Preprint, SPE. Later Published In 1969 In Journal Of Petroleum Technology, V. 21, No. 6, P. 775–786
27. Coates, G., et al., 1997, A New Characterization Of Bulk-Volume Irreducible Using Magnetic Resonance, Paper QQ, 38th Annual SPWLA Logging Symposium Transactions, 14 P. Also Published In 1997 In Dialog (London Petrophysical Society), V. 5, No. 6, P. 9–16. Later Revised And Published In The Log Analyst, V. 39, No. 1, P. 51–63.